Control of an air pressure actuated disposable bioreactor for cultivating heart valves

Control of an air pressure actuated disposable bioreactor for cultivating heart valves

M.J. (Maarten) Beelen
CST 2010.032

Report of Master open space

Supervisory committee:

Ir. P.E. Neerincx[1]
Prof. dr. ir. H.E.H. Meijer[1]
Dr. ir. M.J.G van de Molengraft[2]
Prof. dr. ir. M. Steinbuch[2]

[1] EINDHOVEN UNIVERSITY OF TECHNOLOGY
DEPARTMENT OF MECHANICAL ENGINEERING
POLYMER TECHNOLOGY GROUP

[2] EINDHOVEN UNIVERSITY OF TECHNOLOGY
DEPARTMENT OF MECHANICAL ENGINEERING
CONTROL SYSTEMS TECHNOLOGY GROUP

Eindhoven, September 2010

A personal message

from the author

Although only in the first part of my master Mechanical Engineering, I already had the opportunity to work on two motivational projects, involving a nuclear fusion reactor and a bioreactor. What motivates me is what they have in common. Albeit a great scientific challenge, nuclear fusion has the potential to become a huge contribution to our sustainable energy supply. Some major advantages are the 'fuel' that is abundantly present on earth, the minimal nuclear waste, no emission of greenhouse gasses and its nonexplosive character. A bioreactor for cultivating tissue engineered aortic heart valves could help enabling medical treatments for many patients and significantly improve their well being compared to conventional heart valve replacements.

These goals are grand, the contributions seemingly small.

As every person part of society, a mechanical engineer can purposely choose what goals to devote his efforts to, especially judging from technology's key role at present. Although many of world's problems are much debated and complexified, often endeavors can simply be brought down to being either destructive or constructive. Shortsighted or broad visioned. Weapon intelligence or refugee shelters. Oil depletion or alternative energy sources. Smart bullets or medical innovations.

Although some contributions might seem small, depreciating one's influence takes away one's responsibility. Not a single individual can achieve these goals. With enough of us committed, we might just accomplish them.

Maarten J. Beelen
m.j.beelen@student.tue.nl
September 17, 2010

Abstract

Tissue-engineered heart valves, cultured from human stem cells, are a possible alternative for replacing failing aortic heart valves, where nowadays biological and mechanical heart valves are used. Growing and conditioning is done by mechanically stimulating the tissue in a bioreactor. The disposable injection molded bioreactor [24] uses flexible membranes and steering valves to mimic a physiological heart cycle. In this work, an air pressure actuation control system for this bioreactor is designed. One membrane is position controlled to achieve a desired flow through the heart valve, while another membrane controls the aortic pressure. A third actuator controls a steering valve used to impose a resistance on the flow back to the first membrane, in order to control the heart valve closing pressure. Due to the repetitive character of the setpoints, iterative learning controllers are implemented. A high position tracking performance is achieved and pressure setpoints are mimicked successfully, but the main focus is on preventing large pressure oscillations and other events that could be damaging for the tissue heart valve. The control system allows full adjustability of operating conditions needed for the growing, conditioning and testing phases.

Contents

CHAPTER ONE

Introduction

1.1 Aortic heart valve disorders

The human heart provides a continuous blood circulation through the cardiac cycle. The heart consists of two upper chambers, the left and right atria, and two lower chambers, the left and right ventricles. During systole, the ventricles contract, pumping blood through the body. During diastole, the ventricles relax and fill with blood again. The right ventricle pumps blood into the pulmonary circulation for the lungs, and the left ventricle pumps blood into the systemic circulation through the aorta to the different organs of the body.

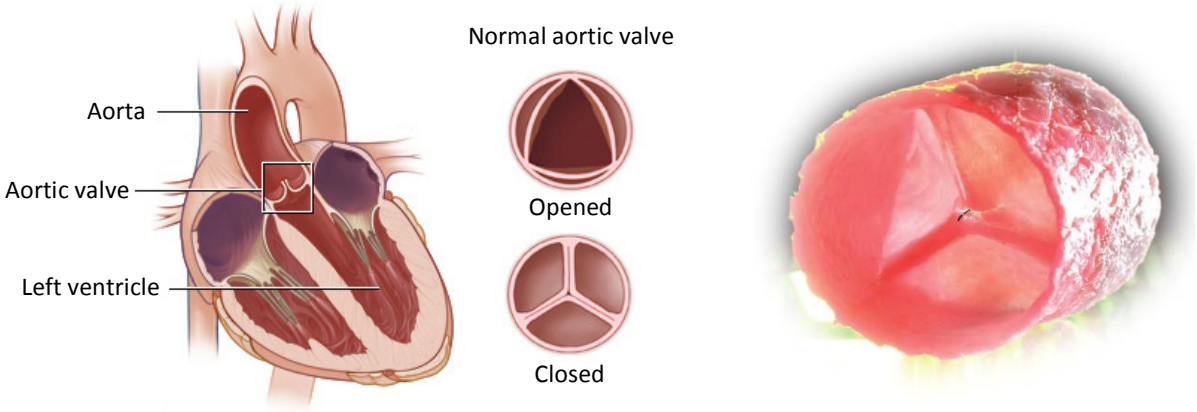

Fig. 1.1: Human heart with aortic valve (left) [16],
example of a tissue engineered heart valve (right) [5]

The human heart is equipped with four types of valves, which prevent blood flow back between strokes. The valve lying between the left ventricle and the aorta is called the aortic valve (Fig. *1.1*). This valve usually consists of three leaflets. There are two conditions that can affect the performance of the aortic valve, aortic stenosis (AS) and aortic regurgitation (AR). AS is caused by incomplete opening of the aortic valve. The valve becomes narrower than normal, impeding the flow of blood. AR is the leaking of the aortic valve, causing blood to flow back in reverse direction. Annually, 6000 children are born in Europe with these heart valve diseases, needing a heart valve replacement.

Nowadays, patients that suffer from AS or AR are treated by surgically replacing the aortic valve by an artificial one, which can be a biological or a mechanical valve. Biological valves are valves from animals, most often from a pig, since a pig heart is most similar to the human heart. There are some risks associated with implanting a biological valve, such as the human body's tendency to reject foreign tissue. Also, the biological heart valve has a limited lifetime. Mechanical valves can last multiple life times, but current mechanical heart valves all require lifelong treatments with blood thinners, to prevent blood clothing. Another drawback of both valve replacements is that they are unable to grow with the patient.

An alternative for biological and mechanical heart valves are cultivated, tissue-engineered heart valves [1][2][7][8][5][22]. An attractive promise of these 'living' tissue replacements is their potential for repair, adaptation and growth. Human stem cells are seeded into a biodegradable artificial structure (scaffold). Culturing the tissue (growing and conditioning) is done by mechanically stimulating it in a bioreactor.

1.2 Recent developments

Recently much research has been done on the subject of Tissue Engineering by various research groups, including the group *soft tissue Biomechanics & Tissue Engineering*, department of Biomedical Engineering, Eindhoven University of Technology. From their experience with cultivating heart valves, the need for a new kind of bioreactor arose, since existing bioreactors have drawbacks. These bioreactors consist of a large number of parts and they are either aimed at controlling the flow through or the strain of the heart valve, not both. Moreover, they are incapable of handling the testing phase of the cultivated valve. Therefore, a new bioreactor has been developed at *the polymer technology group*, department of Mechanical Engineering, Eindhoven University of Technology [24]. This bioreactor is fabricated using injection molding, a technique well suited for mass production. This advantage and others will be further discussed in chapter 1.

In [17], the author designed a feedback system for a prototype of the bioreactor (developed by milling and turning operations) that used linear moving motors as actuators. The problem with this set-up was that pressure oscillations could not be avoided. Since pressure control is crucial, a different approach is preferred for this project. Actuation of the system by means of air pressure is chosen, because of its flexibility, simplicity and reliability.

1.3 Project goals

The purpose of the bioreactor is cultivating tissue into well constructed heart valves, by means of mimicking the cardiac cycle. Three quantities are important in this cycle, with respect to the aortic valve. The pressure in the aorta (P_{ao}), the left ventricle pressure (P_{lv}) and the flow (Q) through the heart valve (Fig. 1.2). Derived from these quantities is the pressure difference over the valve $dP = P_{ao} - P_{lv}$ that builds up when the aortic valve closes during diastole, which is especially important to be imitated correctly. The bioreactor must be able to handle both the cultivating phase and the testing phase. During cultivation, the operating conditions are gradually increased as the tissue grows stronger. For the testing phase, the bioreactor must be able to handle large pressures and volume displacements up to $80\ mL$ per cycle, and maximum flows of $600\ mLs^{-1}$.

Main project goal

" To design and realize a feedback control system for the disposable bioreactor achieving all necessary functionality for cultivating aortic heart valves "

At the time of this writing research is being conducted to find the optimal mechanical stimulation protocol for cultivating heart valves. Therefore, the exact performance requirements for the control system are not yet known entirely. However, the desired 'necessary functionality' can be formulated using these qualitative goals:

- Mimic the physiological cardiac cycle, focusing on the aortic pressure, the left ventricle pressure and the flow through the heart valve, by means of air pressure actuation
- Suppress pressure noise near the heart valve
- Full adjustability of setpoints and operating conditions through a user interface
- Safety system to respond to (or prevent) events that can cause tissue damage
- Robustness to leakage, relaxation and other system changes, in order to provide the durability for several weeks non-stop operation
- Gradual system startup and gradual change of working conditions in response to abrupt setpoint changes by user
- Multi protocol support, e.g. automatic nutrient fluid ventilation and refreshment
- Real time monitoring of pressure and flow signals and on demand signal logging
- Heart valve visualization and video capturing using a high speed camera

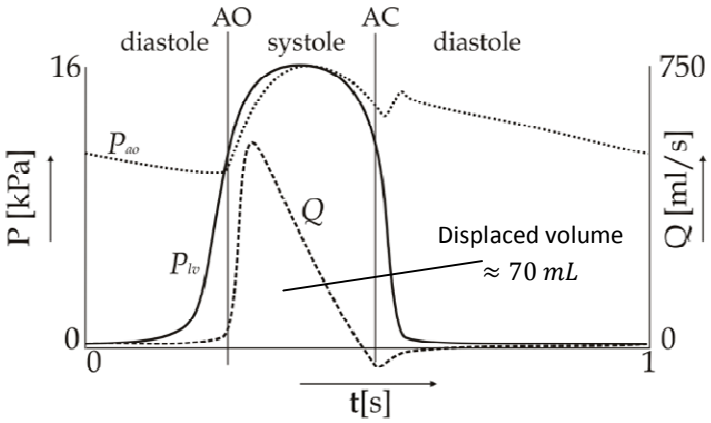

Fig. 1.2: Typical physiological pressures (P) and flow (Q) during the cardiac cycle

CHAPTER TWO

System set-up

In this chapter, the bioreactor set-up is described. A distinction is made between disposable parts (section 2.1) and reusable parts (section 2.2). Three different disposable parts are injection molded (bioreactor shells, pressure caps and clips) [24], while tubes and other appendices are purchased. The reusable part of the set-up includes the data acquisition system (DAQ), sensors, actuators and the pneumatic system. Two identical bioreactor shells together with two pressure caps, clips, tubing and sensors compose the bioreactor assembly (Fig. 2.1). This assembly will be placed in its entirety inside an incubator.

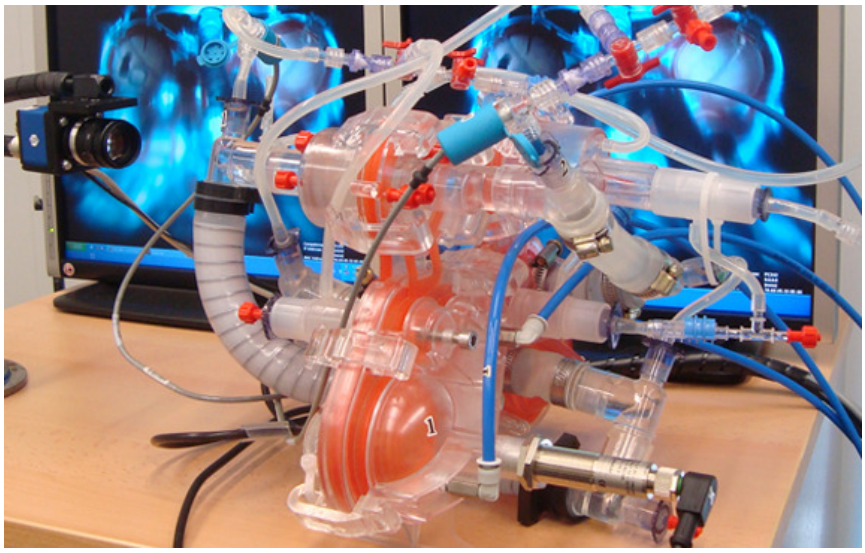

Fig. 2.1: Bioreactor assembly with tubes and sensors

2.1 Disposable parts

The bioreactor consists of two identical line-symmetric shells that are assembled together (Fig. 2.2). A shell is fabricated using two component injection molding on the Ferromatic K-tec 60 injection molding machine, available in the laboratory [19]. Each shell consists of a hard (polycarbonate (PC)) and soft component (thermoplastic polyurethane (TPU)) and is molded using four injection shots in two mold positions, using a rotating mold. The soft component (red in Fig. 2.4) is used for a sealing between the two shells, for a membrane that acts as a bellows to pump the fluid inside the bioreactor and for steering valves (Fig. 2.3).

A pressure cap (Fig. 2.5) is mounted over the bellows and steering valves, and is fixed using injection molded clips (Fig. 2.5). These clips are also used to fix the bioreactor shells together, and to firmly close the chamber that is used to mount the heart valve in and the chamber for nutrient fluid supply. (The parts of the bioreactor that are in contact with nutrient fluid have to be sterilized on beforehand, and disposed of after use. The sealing clip and pressure caps do not come in contact with the nutrient fluid, so strictly speaking, they can be reused.)

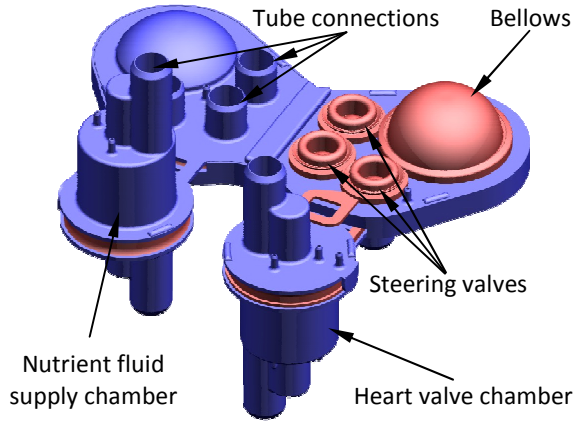

Fig. 2.2: CAD model of two identical shells assembled [24]

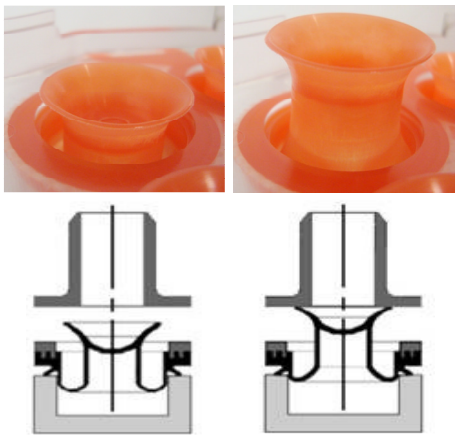

Fig. 2.3: Steering valves
Open position (left), closed position (right)

Fig. 2.4: Injection molded bioreactor shell

Fig. 2.5: The sealing clip (upper) and the pressure cap (lower)

The steering valves have a low stiffness in vertical direction, and can therefore be pushed down easily by controlling the actuation pressure between the pressure caps and the steering valves. When a steering valve is pushed down, it closes on its corresponding tube-connection, see Fig. 2.3. By controlling the closing force of the steering valve, resistance can be imposed on the flow through the tube connection. This method will prove to be useful (in chapter 4) to actively control pressure drops over the tissue engineered heart valve.

The membrane that acts as a bellows to pump the fluid inside the bioreactor is also air pressure actuated. The bellows is dented using an actuation pressure between the pressure cap and the bellows. The position of the midpoint is measured contactless using an ultrasonic sensor. Using this position, the displaced volume is calculated. The ultrasonic measurement fails when the normal at the midpoint location is not properly aligned with the sensor, due to asymmetric deformation of the bellows. As a result, the sound wave travels a longer path until it is observed by the sensor. Therefore, this event is characterized by large peaks in the position measurement. The first bellows-design has a spherical geometry. Due to residual stresses and imperfections in the membrane, it tilts during deformation, see Fig. 2.6 (left). This causes the position measurement to fail dramatically, and closed loop control on the position is often not possible. An effort to resolve the problem was made by enhancing the membrane with ribs. Because the buckle in the membrane is five parted, also five ribs were placed to allow this natural deformation. The ribs increase in thickness from the center to the edge of the sphere. When, during asymmetric deformation, one buckle becomes bigger than others, it is subject to more resistance. In this way, a restoring force is applied to make the symmetric deformation the preferred one. This resulting second bellow-design is slightly better but not sufficient. The solution was found in molding the membrane not in its outer position, but in its neutral position, in-between the maximum and minimum volume stroke. The improved membrane has a wavy geometry, to allow large volume strokes, and a flat surface in the center to allow easy ultrasonic position measurement. Dimensions like the radius and wall thickness of the curls are optimized in order to maximize the stabilizing force, i.e. a reaction force that follows from slightly offsetting the midpoint of the membrane [24]. More properties of this membrane are described in chapter 3.

Since a real tissue heart valve is valuable and vulnerable, a thin, three leaflet TPU test heart valve [12] is used during demonstrations, system identification of the bioreactor, and other experiments with the feedback control system. Other disposable parts such as tubes, connectors, clamps, checkvalves and dead-enders are purchased from medical component suppliers such as Qosina [29].

Fig. 2.6: Buckling of the three different bellow designs
The first spherical membrane (left), the spherical membrane enhanced with five ribs (center) and the final membrane with a curled, wavy geometry (right).

2.2 Reusable parts

In this section, the choices for the feedback system are explained. At first, an experimental prototype feedback system was established; later the entire system set-up was reproduced four times. The bioreactor set-ups are available for demonstrations, experiments and most importantly, for laboratories that are performing research on cultivating heart valves.

2.2.1 Sensors and actuators

The pressure difference before and after the heart valve is measured using miniature reusable pressure transducers from Becton Dickinson [3], that have a pressure range of -4 to $40kPa$ (Fig. 2.7). The sensors are mounted inside a sterile disposable dome, in contact with a flexible membrane that transmits the pressure from inside the bioreactor, to the sensing diaphragm of the transducer. The dome membrane provides a sterile barrier between the transducer sensing diaphragm and the nutrient-fluid-filled chamber of the dome. In this way, the sensors can be reused and do not have to be sterile. The dome is made from transparent plastic to facilitate the detection and removal of bubbles since even minute bubbles can degrade the frequency response of the pressure monitoring system.

Position measurement of the bellows is done contactless, using ultrasonic sensors from Microsonic [21] (Fig. 2.7). They are mounted inside the injection molded pressure caps, aligned with the surface normal of the bellows at the mid-point location, and with a minimum distance of $30mm$ to the bellows, such that the bellows is always in the sensor's detection zone. The fact that the pressure in the chamber is constantly changing has no influence on the measurements, since the velocity of sound is only proportional to the square root of the temperature, and the sensors are equipped with an internal temperature compensation. The sensors have an accuracy of $0.2mm$, and the sound-beam is narrow enough to focus on the midpoint of the bellows. The sensors are programmed to output an analog signal of $1V$ per $10mm$ displacement.

Air pressure actuation is performed via electronic proportional air flow valves from Festo [10] (Fig. 2.7). Two different types are used, a proportional pressure regulator (MPPES series) and a proportional directional control valve (MPYE series). The MPPES has been designed for regulating the output pressure proportional to a specified electrical nominal value, and therefore contains an internal control circuit.

Fig. 2.7: Pressure sensor with disposable dome [3], ultrasonic position sensor [21], proportional pressure regulator (MPPES), proportional directional control valve (MPYE) [10]

Because the output pressure of this actuator is thus known, it is used to control the steering valve in the bypass, since the desired actuation pressure is often a function of the internal pressure in the bioreactor. The MPPES has a fairly slow, but very smooth step response. It is preferred above an actuator from Norgen [25] that has the same working principle, but with a fast but noisy step response.
The MPYE air flow valves are used for actuating the bellows. In this case, the actuating pressure does not need to be known, since the control objectives are the position of the bellows, and the internal bioreactor pressures. The MPYE controls a valve opening (5/3-way function) proportional to an input voltage. Connecting compressed air to one supply port, and vacuum air to another, an extremely fast and smooth step response is obtained using this valve.

The pneumatic system is connected to compressed air in the laboratory, and consists of the four before mentioned air flow valves, an air filter, tubing, air reservoirs to provide a supply of compressed air for fast pulses and to compensate pressure fluctuations, and an oil lubricated vacuum pump from Horst-Witte [15]. This pump has an end vacuum rate of $0.1mbar$ absolute and 10 m^3/h suction capacity, see Fig. 2.8.

2.2.2 Real-time data acquisition system

The real-time Data Acquisition (DAQ) system consists of a PC running on windows, with an internal multifunctional PCI DAQ card from National Instruments [23]. Using two connector blocks (Fig. 2.8), all sensors and actuators are connected to this PCI card, and to a $24V$ DC power supply. The PCI card was selected for our application because it provides four 16-bit analog outputs. Furthermore it has 32 analog inputs and 48 digital ports that can be programmed to be inputs or outputs. Another advantage of this card is the availability of a driver that enables integration in Real-Time Windows Target [20], a toolbox from Matlab. This toolbox enables Simulink models to run in real-time on a PC, driving the hardware-in-the-loop control system. The Real-Time Workshop generates C code and creates a binary file using the supplied compiler. The resulting file is loaded into an external mode kernel, and a connection with Simulink is established, enabling data logging, signal viewing and the tuning of model parameters in real-time. The bioreactor-Simulink-model is running with a sampling frequency of 1 kHz, which is fast enough for this fairly slow control problem. The explicit fixed-step continuous solver used is *ode5*, a fairly complex but accurate solver available in Matlab, since the computational demands can be met using a modern PC.

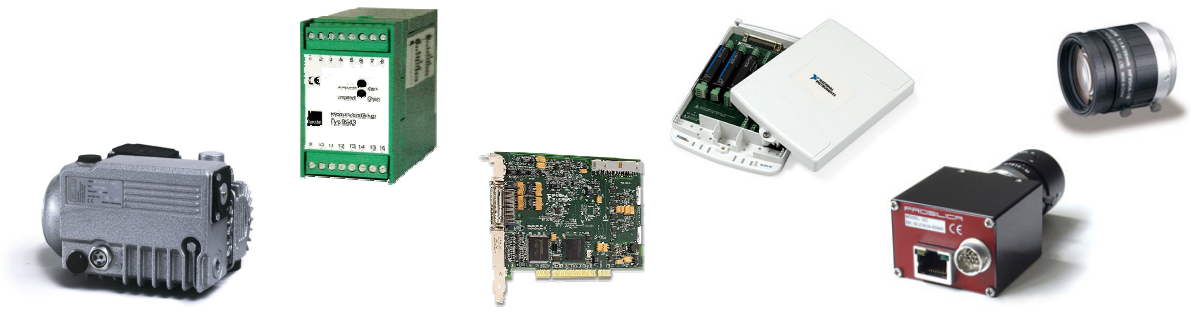

Fig. 2.8: Vacuum pump [15], single channel amplifier module [6], PCI DAQ card [23], connector block for hardware, high speed camera [28] and 35 mm lens [11]

The analog output signal of the pressure sensors is very low, and has to be amplified to a standard signal of $0 - 10V$. In the early stages of the project, this was done using the Picas Measuring Amplifier [27] from Peekel Instruments. When reproducing the feed-back system, a cheaper and more compact alternative was found, and the Picas was replaced by two single channel amplifier modules from Burster [6]. These modules have an accuracy of 0.05%, and are fine tuned using a potentiometer.

For visualization of the cultivating heart valve, a high speed color camera from Prosilica [28] films through the transparent heart valve chamber of the bioreactor. The camera runs 200 frames per second at VGA resolution (640x480), over its Gigabit Ethernet interface. A 35mm lens from Fujinon [11] is used to focus on the heart valve. Observing the heart valve provides an intuitive understanding on how the physiologically conditions are achieved. It provides a tool for visual inspection of the closing of the valve. In the future, the camera will not only be used for observation by the end-user, but also for automatic image analysis in the loop. A method was developed [18] to estimate the heart valve deformation and other mechanical properties, by looking from a top-view on the heart valve. Based on these properties, resulting from the cultivation process, the setpoints for the cardiac cycle pressures and flow (Fig. 1.2) could be gradually changed during cultivation.

2.3 Working principle

A schematic representation of the bioreactor's working principle is provided in Fig. 2.9. The objective is to mimic physiological conditions like the example of Fig. 1.2. Bellows 1 acts as the driving membrane, and is controlled on its position. By integrating the desired flow (Q) through the heart valve, the volume displacement is obtained, and consequently the setpoint for the position of bellows 1 is calculated. In general, bellows 2 is used to control the aortic pressure (P_{ao}). During the systole phase of the cardiac cycle, when the aortic heart valve is open, the bypass steering valve is entirely closed by using an actuation pressure equal to P_{ao} plus an additional valve closing pressure. In this way, all fluid-medium displaced by bellows 1 is forced through the heart valve. During diastole, the aortic heart valve closes, and the nutrient-fluid is pumped back to bellows 1 ('the left ventricle') through the bypass. The bypass valve is used to impose a resistance on this flow back, in order to control the heart valve closing pressure $dP = P_{ao} - P_{lv}$.

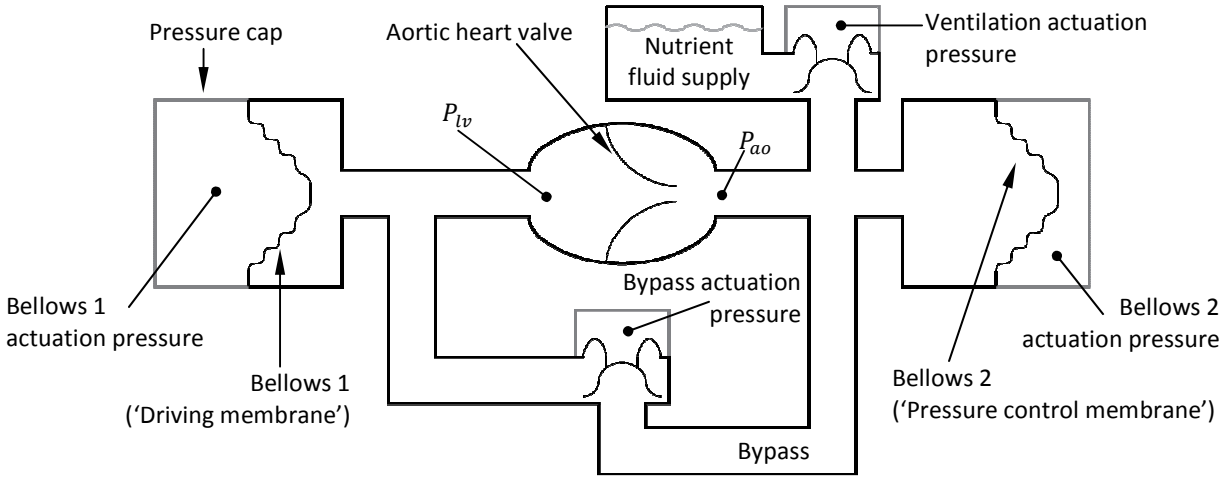

Fig. 2.9: Schematic representation of the working components during flow through the bioreactor (diastole phase)

CHAPTER THREE

Bellows position control

Before addressing the multi-input multi-output (MIMO) control problem, the single-input single output (SISO) system that results from controlling a single bellows on its position is investigated in this chapter. It provides a basis to develop control strategies and allows for intuitive understanding of the system properties. From a control point of view, the bellows is the most important component of the bioreactor. In section 3.1 some geometrical properties of the bellows are described, and the transfer function is identified. The loop is closed in section 3.2, where controllers are shaped, feedforwards tuned, and an on-line iterative learning control algorithm is proposed. For the experiments described in this chapter, the bioreactor is emptied from nutrient fluid, and opened to the outside world, in order to isolate the behavior of the bellows and eliminate other influences.

3.1 System identification

In this section, the behavior of the bellows is identified by looking at its deformation geometry, analyzing its damping behavior using a pressure-volume diagram, and by analyzing it in the frequency domain.

3.1.1 Deformation geometry

The ultrasonic sensor measures the position of the surface midpoint of the bellows, i.e. the bellows indentation h. Not this position, but the flow Q is a control objective, which is the derivative of the displace volume V. Therefore we propose a model to describe the relation $V(h)$. The undeformed membrane has base radius R. When it is deformed such that the indentation h of the membrane is equal to this radius, it resembles a hemisphere with volume $V = 2/3\pi R^3$, see Fig. 3.1a. When the indentation is not equal to this radius, the bellows can be modeled by a hemisphere that is deformed in vertical direction with factor h/R, see Fig. 3.1b. Since a quarter circle is described by the relation $y = \sqrt{R^2 - x^2}$, the right half of the deformed hemisphere curvature is described by $y = \frac{h}{R}\sqrt{R^2 - x^2}$. Revolving the area under this curvature around the y −axis results in the body that describes the deformed bellows. Taking the infinite sum of all cylindrical shells in the domain $\{0, R\}$ results in the body's volume

$$V(h) = 2\pi \int_0^r xydx = \frac{2\pi h}{R} \int_0^r x\sqrt{R^2 - x^2}dx = \frac{2}{3}\pi R^2 h\,. \tag{3.1}$$

Luckily, the result is a linear relation between the position and the displaced volume. The relation can be interpreted as a cylinder with the same base radius and height $2/3h$. This simplified model does not take the wavy geometry into account, but measurements verified the model provides an accurate representation. The base radius of the membrane $R = 30mm$. The membrane touches the pressure cap at $h \approx -18mm$, defining the most inward position, while the most outward positions $h \approx 35mm$ is defined by the bioreactor shell. Therefore the maximum volume stroke of the bioreactor is $V \approx 100mL$, but to prevent aggressive actuation pressures, normally a stroke of $V = 80mL$ is not exceeded.

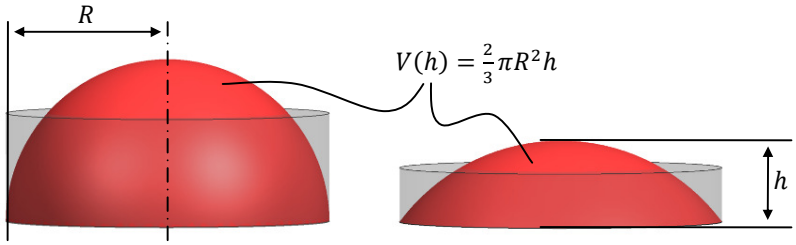

a) $h = R$ (hemisphere) b) $h < R$ (compressed hemisphere)

Fig. 3.1: Bellows deformation geometry

3.1.2 Pressure-volume diagram

For this experiment, the bellows is position controlled, with a simple Proportional-Integral (PI) controller, to follow a sinusoidal setpoint around its undeformed position, for 10 cycles. The required actuation pressure as a function of the bellows volume is displayed in Fig. 3.2, for three different cycle times. Each loop is formed in clockwise direction, and the area enclosed by the graph resembles the energy dissipated in the cycle. For low cycle times, a high actuation pressure is needed, and the work done by the system is large. The figures visualize the damping and the nonlinear behavior of the bellows. Only for very slow cycles ($> 10\ s$), the graphs of the inward and outward stroke almost coincide, and are fairly linear on the domain between $-40mL$ and $+40mL$. The actuation pressure needed to keep the bellows in the $+40\ mL$ position is $7kPa$, characterizing the stiffness of the membrane.

In cardiovascular physiology, to characterize the heart's performance, the PV diagram is often applied to the left ventricle. The left ventricular pressure is plotted as a function of the left ventricular volume. The bellows in the bioreactor that is position controlled actually resembles this left ventricle. The difference for the real heart PV diagram is that both axes are reversed, and the cycle is formed in anti-clockwise direction, since not the actuation pressure (needed 'to drive the heart') is plotted, but the left ventricle pressure ('delivered by the heart'). Also figure Fig. 3.2 displays the volume displaced by the left ventricle, which is reverse of the volume inside the left ventricle.

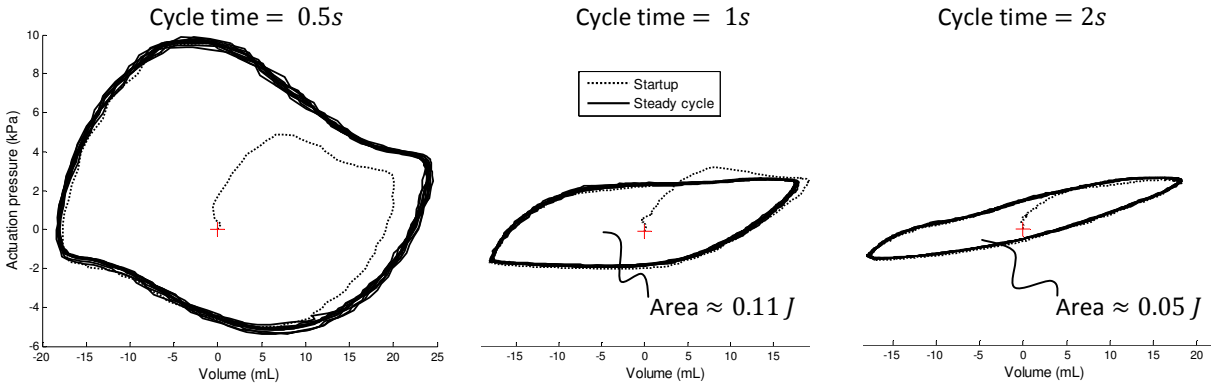

Fig. 3.2: P-V diagrams

3.1.3 Frequency domain

The dynamic behavior of the bellows is identified using an experiment. White noise is injected as input signal for the actuator, and the response in the position of the bellows is measured, and saved using Simulink. The resulting Frequency Response from the actuator input to the position of the bellows is displayed in Fig. 3.3. Judging from the coherence, the measurements are only accurate up to 5 Hz. For higher frequencies, the ultrasonic sensor (resolution $= 0.08mm$) fails to measure the small position response accurately. A damping behavior is recognized since the magnitude shows a minus one slope, and the phase delay is 90 degrees. Fitting a transfer function results in $H(s) = 42/(\mathrm{s} + 1.3)$.

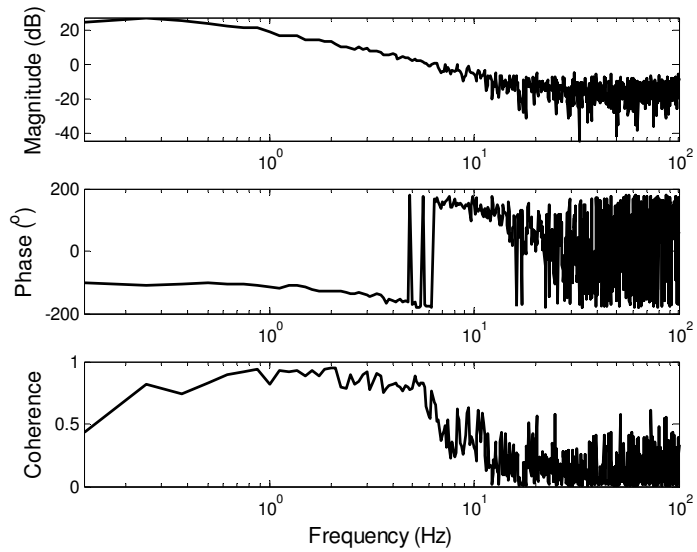

Fig. 3.3: Bode plot for Bellows1
From actuator input (V) to response in bellows position (mL)

3.2 Position control

In this section, a position controller for the bellows is developed. Before using the setpoint from the cardiac cycle, a second degree setpoint with a stroke of $40mL$ is used that is convenient for tuning controller parameters and feedforwards. The position controller is constructed from a Proportional-Integral (PI) controller, feedforwards based on a delayed reference signal (section 3.2.2), and an Iterative Learning Control algorithm (section 3.2.3). The performance of these control strategies is tested using an experiment, see Fig. 3.4. The experiment consists of several events, where the separate controllers and combinations of controllers are tested. The events are further explained in the following sections.

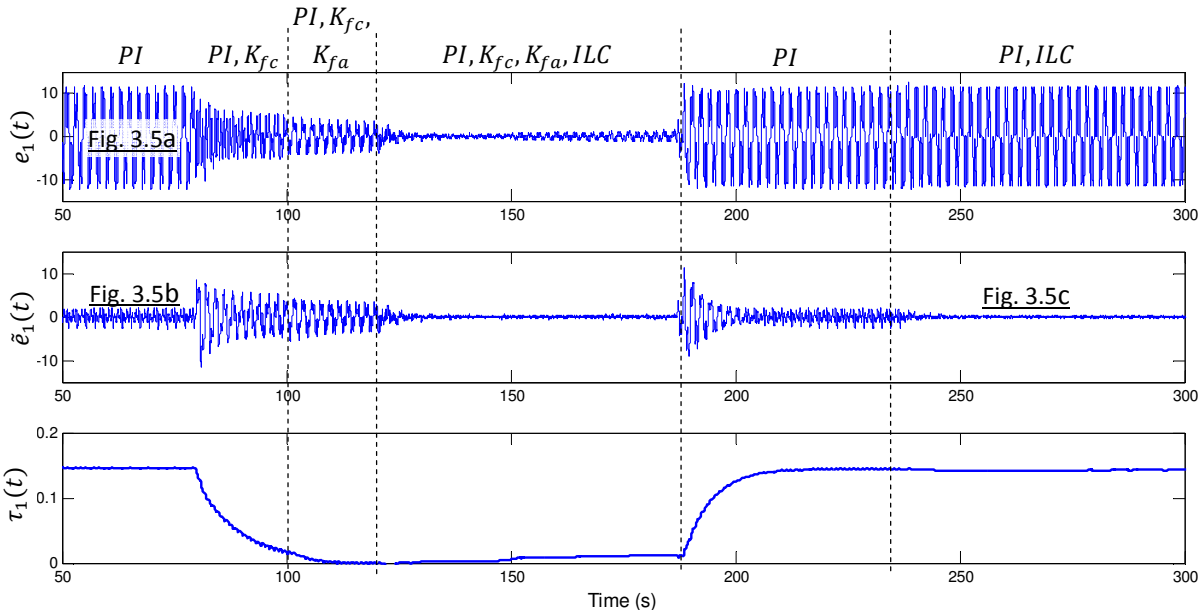

Fig. 3.4: A position control experiment using automatic estimation of the delay $\tau(t)$, and the influence of the different controllers on the errors e_1 and $\tilde{e}_1$.

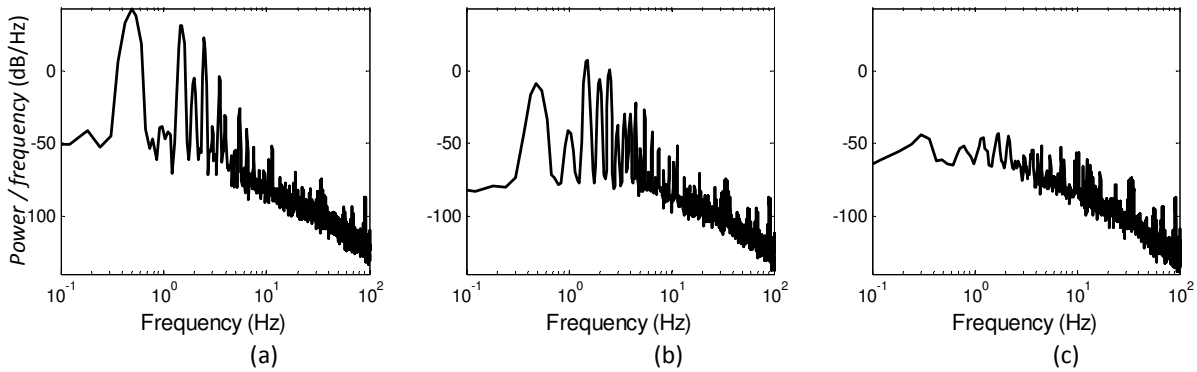

Fig. 3.5: Power spectral density estimates of the PI controller errors $e_1(t)$ (a) and $\tilde{e}_1(t)$ (b), and the error $\tilde{e}_1(t)$ resulting from the PI and ILC controller

3.2.1 Shaping the SISO controller

Because the position measurements are not very smooth, derivative control gives rise to large vibrations in the system and is therefore not useful, even when a lowpass-filter is added in the feedback path. We start by tuning a Proportional-Integral (PI) controller using loop-shaping, in order to obtain an open loop with a cross-over frequency of 1Hz. , The bode diagram of the open loop (Fig. 3.7a) shows a 60° phase margin at this frequency. The Nyquist diagram (Fig. 3.7b), shows a gain margin of 7.1 and a modulus margin of 0.75, hence the closed loop is stable. The resulting controller parameters, {P, I} = {0.12, 0.05}, are implemented and tested, see $t = 50$ in the experiment (Fig. 3.4). The most dominant frequency in the position error is 0.5Hz, see the power spectral density plot in Fig. 3.5a.

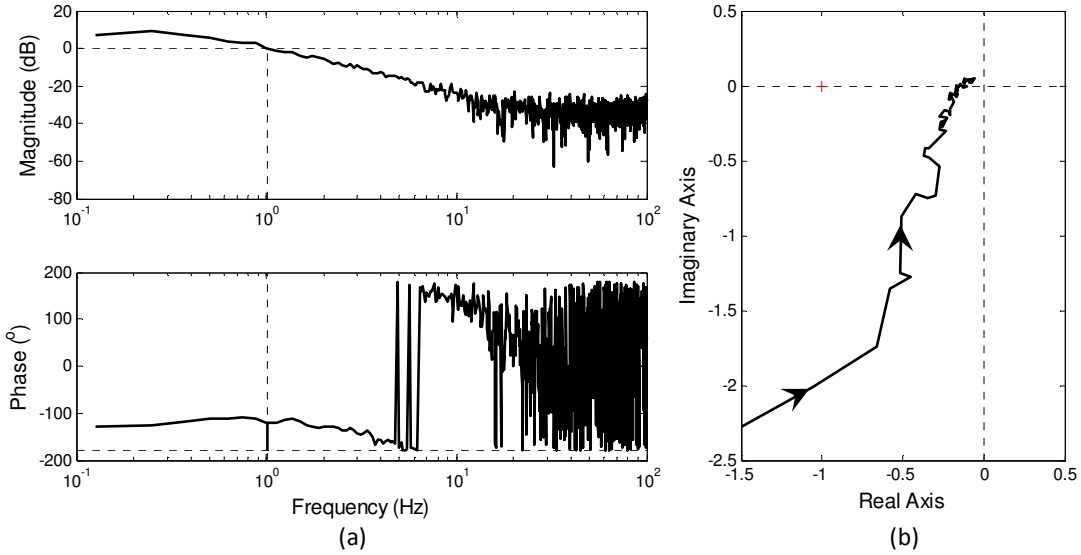

Fig. 3.6: Bode diagram of the open loop (a) and Nyquist diagram (b)

3.2.2 Automatic delay estimation

The delay in the system is considerable ($0.14s$ at $t = 50$), due to the phase delay of the controller, the dynamics of the sensor, actuator, electronics and the pneumatic system. It is not important at what time the system produces a certain output, as long as it resembles the cardiac conditions. Therefore, the system is allowed to have this delay. The error $e_1(t)$, the difference between the original reference signal $r_1(t)$ and the measured output $y_1(t)$ is large (Fig. 3.4 top), but the error $\tilde{e}_1(t)$ that is based on a delayed reference signal $\tilde{r}_1(t)$ is much smaller (Fig. 3.4 center). The reference $\tilde{r}_1(t) = r_1\big(t - \tau_1(t)\big)$ results from delaying the original reference with $\tau_1(t)$ seconds. This variable delay is estimated on-line, in order to optimally fit the new reference on the measurements, i.e. to minimize $\tilde{e}_1(t)$. This is done by subdividing the setpoint in strictly monotonically increasing parts, and strictly monotonically decreasing parts. During increasing parts, when the shifted reference $\tilde{r}_1(t)$ is above (below) the measured signal, the delay $\tau_1(t)$ is increased (decreased). Vice versa for decreasing parts. Using an integrating action and gain K_{τ_1}, the delay $\tau_1(t)$ is determined, and hence $\tilde{e}_1(t) \leq e_1(t)$, $\forall t$. We note that, during the first part of the experiment, this delay calculation has no influence on the output $y_1(t)$, since the PI-controller is based on the original reference signal.

To improve performance, feedforward control is added. Tuning the feedforward K_{fc}, a feedforward for eliminating friction, results in $K_{fc} = 0.7$. When it is enabled at $t = 80$, it reduces the error e_1. The velocity feedforward K_{fv} should reduce the error at constant speed sections, but it provides no improvement. The mass feedforward $K_{fa} = 4 \cdot 10^{-4}$ is added at $t = 100$, further reducing the error e_1. As a result of the feedforward, the delay in the system decreases, and almost vanishes, i.e. $\tau(110) \approx 0$. However, the more important error $\tilde{e}_1(t)$ actually increases, and therefore, these feedforwards are unwanted.

An important objective is to realize the volume strokes that are prescribed. When a weak controller is used, the required stroke is often not realized. Especially when the internal bioreactor pressure is high, the position control becomes more difficult. Therefore, an algorithm is incorporated that observes the realized stroke after each cycle, and compares it to the prescribed stroke. The error is integrated with gain K_κ, resulting in a correction factor $\kappa(t)$, that multiplies the original reference signal, i.e. $\hat{r}_1(t) = r_1(t)\kappa(t)$. When the volume stroke is insufficient, the system feeds an elongated setpoint signal into the PI-controller. In this way, the stroke is always exactly matched, and does not have to be monitored manually. However, stability of this method is hard to predict. Therefore, a different strategy to make the proper corrections is chosen, which is described in the following section.

3.2.3 Online updating Iterative Learning Control

The setpoints in this control problem are repetitive. Therefore the error shows similar behavior every cycle. This *a-priori* knowledge of the error is used to further improve performance. An Iterative-Learning-Control (ILC) approach is introduced, aiming at reducing the error by entirely eliminating its repetitive part, remaining only with the non predictive part of the error.
At setpoint cycle k, the error $\tilde{e}_k$ is recorded during the entire cycle, and used to update the ILC signal f_k which is played back as a feedforward during the sequential cycle. Since the system dynamics change at every system restart, due to numerous unpredictable outside influences, it is not convenient to update the ILC signal offline, and restarting after each update. Also, when system dynamics change or the setpoint is adjusted, the ILC signal has to be reestablished, and restarting the system is not an option while cultivating heart valves. The solution is to implement an on-line, ever updating ILC. Every cycle is divided in a fixed number of samples. We define the error at the j^{th} sample of cycle k as $\tilde{e}_k^j$, and the corresponding value of the effective iterative learning control signal of the previous cycle as f_{k-1}^j. The ILC signal is updated every sample, with learning rate α, following the update law

$$f_k^j = \left(f_{k-1}^j + \alpha \tilde{e}_k^j\right) L(s), \tag{3.2}$$

where $L(s)$ is a low-pass filter to cut-off high frequencies that are unwanted in the feedforward signal. In fact, $L(s)$ acts as robustness filter that allows constant updating of the ILC signal without the system getting unstable. Another option is to stop updating when the ILC signal converges, (i.e. $f_k^j = f_{k-1}^j$). A trigger can restart the update, e.g. when the user changes setpoints.

In combination with the PI-controller and the feedforwards, the ILC-algorithm is enabled at $t = 120$ (Fig. 3.4), reducing the error with a factor 4. The feedforwards are turned off at $t = 185$, causing the natural

delay time of the system to return, with a rate depending on the integrator gain K_{τ_1}. Similar to the experiment start, the system operates with only a PI-controller. The largest part of the error is repetitive and clearly visible, see Fig. 3.7. The maximum absolute error $|\tilde{e}_1(t)| \approx 2.7\ mL$. The ILC-algorithm is enabled again at $t = 235$, and the repeating errors are successfully suppressed; the maximum error is reduced with a factor 7, to $0.37\ mL$. The learning rate $\alpha = 0.1$ causes the system to establish a steady ILC signal within a few setpoint cycles.

Automatic Delay Estimation is used for correct error estimation when only the PI-controller is used. In combination with the ILC however, the use of the delayed reference signal shows a more important role. Basing the ILC on the original setpoint would force the system to have zero delay. The natural delay of the system is kept intact by introduction of the Automatic Delay Estimation, allowing the ILC and PI controller to work in parallel.

More results from position control experiments are provided in appendix B. These experiments are based on the cardiac heart cycle reference, with varying stroke volumes between $10mL$ and $80mL$.

In this chapter a SISO experiment was considered, where the bellows was position controlled, with the bioreactor opened to the outside world. It provided intuitive understanding of the system properties and control strategies were developed.

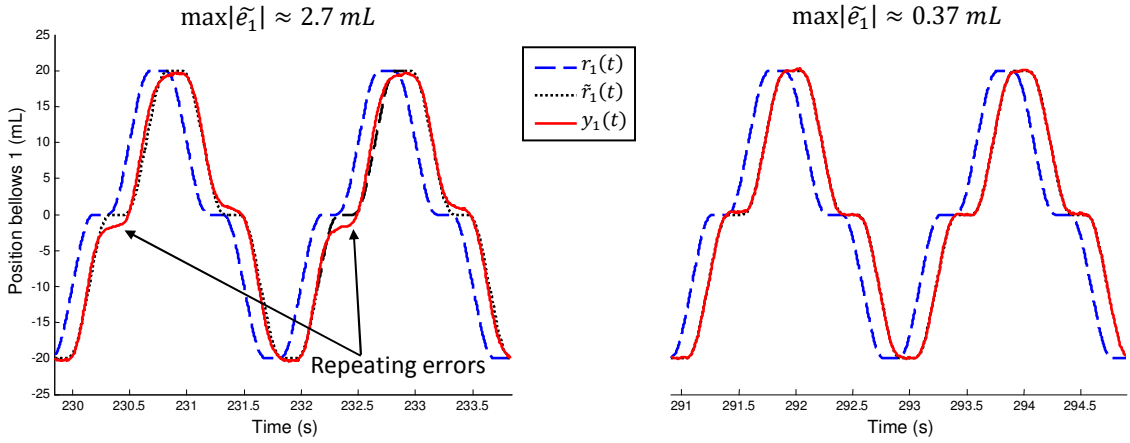

a) PI-controller b) PI-controller + ILC

Fig. 3.7: Performance of the PI-controller (a), compared to the PI-controller in combination with Iterative Learning Control (b), during a position control experiment using a second degree setpoint.

CHAPTER FOUR

Pressure control

Using the knowledge obtained from the SISO experiment in the previous chapter, the MIMO control problem is now considered. The bioreactor is filled with water to simulate nutrient fluid and is closed to the outside world, to allow for internal bioreactor pressure control. A TPU test heart valve as described in section 2.1 is implemented to resemble a tissue heart valve. In section 4.1 transfer functions of the MIMO plant are identified. Feedback controllers and feedforwards for the Aortic Pressure are introduced and evaluated in section 4.2. In section 4.3 the bypass is actuated to control the valve closing pressure, and in section 4.4 all automatic bioreactor functionality is described.

4.1 MIMO plant identification

The MIMO system has 4 inputs and 4 outputs as displayed in Fig. 4.1. A description of these inputs and outputs is given in Table 4.1.

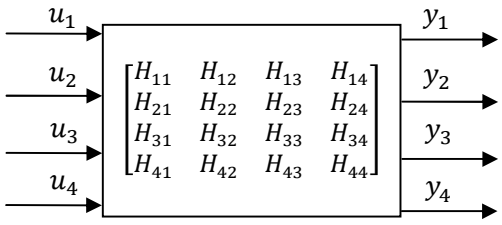

Fig. 4.1: MIMO plant

Table 4.1: Parameters in control architecture

References		Control input actuators		Outputs	
r_1	Position bellows 1	u_1	Bellows 1	y_1	Position bellows 1
r_2	P_{ao}	u_2	Bellows 2	y_2	P_{ao}
r_3	dP	u_3	Bypass	y_3	P_{lv}
		u_4	Ventilation	y_4	Position bellows 2

4.1.1 Frequency domain

To identify the MIMO plant, the dynamic signal analysis system SIGLAB [33] is used. Noise is injected in inputs u_1 and u_2, and all four outputs are measured. Using an internal routine from SIGLAB the transfer functions from the eight corresponding plant entries are calculated.

The plant is highly nonlinear, therefore perturbations around different operating points are considered to be able to do FRF measurements. The transfer functions displayed in Fig. 4.2 resemble a linearized plant where both bellows move around their zero position $(0\ mL)$, while the internal bioreactor pressures fluctuate around $12\ kPa$. The steering valves from the bypass and ventilation are kept open.

Measurements around other operating points were also considered. The plant shows different dynamics when for instance bellows 1 moves around its $20\ mL$ or $-40\ mL$ position, or when another internal pressure is maintained. These results are not shown here however, since the measurements are not very accurate, and we will not used them for the controller design. We will assume the non-linear behavior is small enough to be able to stabilize the system using linear controllers, and see what performance it will give.

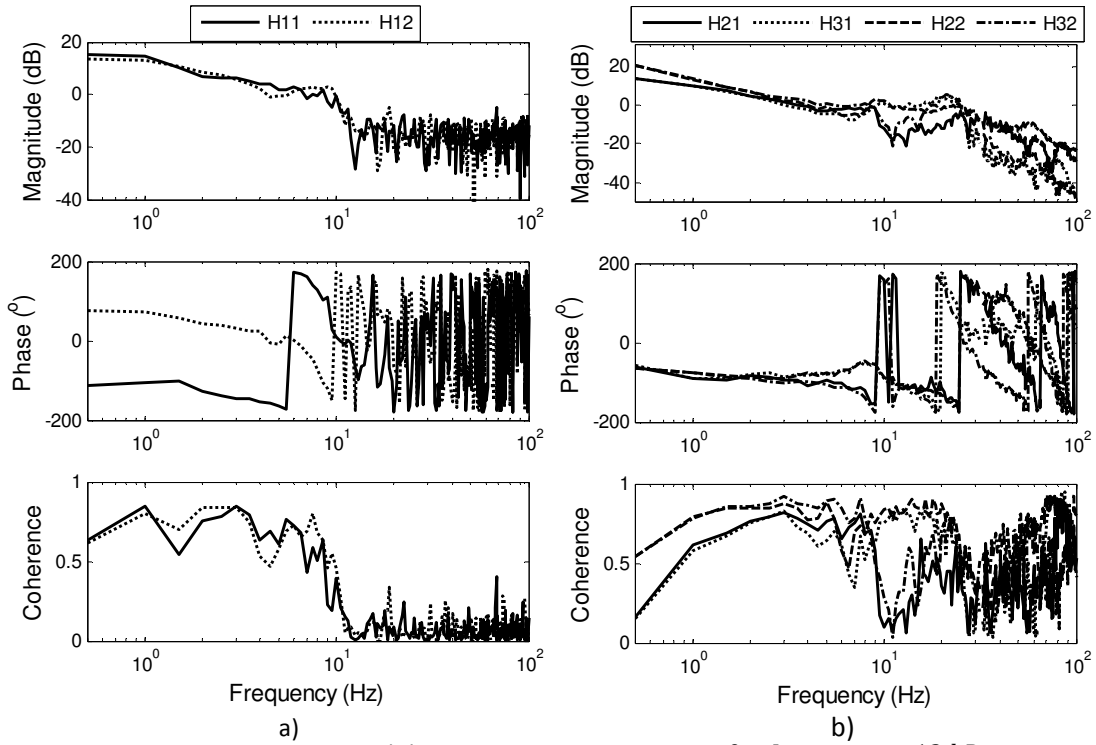

Fig. 4.2: FRF measurements around the operating point $y_1 = y_4 = 0\ mL$, $y_2 = y_3 = 12\ kPa$. From u_1 and u_2 (V) to the position y_1 (mL) (a), and from u_1 and u_2 (V) to the pressures y_2 and y_3 (kPa) (b).

In Fig. 4.2 not all transfer functions are displayed since some symmetry is assumed. For the transfer functions corresponding to the positions y_1 and y_4 we assume that $H_{11} \approx H_{42}$ and $H_{12} \approx H_{41}$. These first two entries resemble direct transfer functions, while H_{12} and H_{41} resemble cross influences (hence the 180° phase difference). The same assumption is made for the direct and cross terms corresponding to the pressures. On top of that, it holds that during systole (when the heart valve is open) $P_{ao} \approx P_{lv}$ and therefore all entries corresponding to pressures are identical. These four transfer functions are shown in Fig. 4.2b, and their differences are due to different bellows, sensor and actuator characteristics. For example, the bode-magnitude plot shows a small difference in the behavior of both bellows. For low frequencies H_{21} approximately coincides with H_{31}, because their low frequent behavior is mainly governed by the bellows 1 behavior. Similarly $H_{22} \approx H_{32}$ for low frequencies. The bellows are not identical due to small imperfections and the injection molding process in general. The control system should take these system uncertainties into account.
The inputs u_3 and u_4 both actuate steering valves, and their influences are highly nonlinear, and coupled to the flow inside the bioreactor. Therefore a transfer function with a reasonable coherence could not be obtained. The coherence of Fig. 4.2a collapses at an even lower frequency than the coherence of Fig. 4.2b. This is due to the limited resolution of the ultrasonic position sensors.

4.1.2 Pressure-volume diagram

Closing the bioreactor from the outside world results in a higher actuation pressure needed to move a bellows, because the entire system has to expand and contract. For comparison, a similar experiment as in section 3.1.2 is performed. Bellows one is position controlled to follow a few cycles of a sinusoidal setpoint, while bellows 2 is used to control the pressure around $12\ kPa$, using a weak integral action.

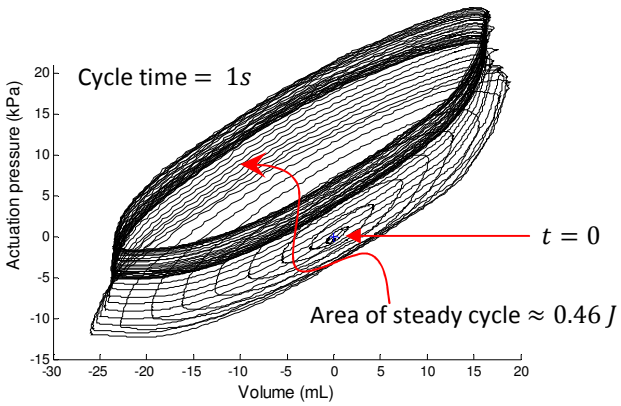

Fig. 4.3: P-V diagram bellows 1, closed system

In Fig. 4.3, the actuation pressure is plotted against the volume displacement of bellows 1. At experiment start (marked with $t = 0$), the sinusoidal setpoint and the internal pressure are gradually increased, until a steady state cycle is reached with an internal pressure of 12 kPa. The rising spiral with increasing radius in the figure indicates the stable build up of the setpoints. The steady state cycle is formed in clockwise direction and has an area of $0.46\ J$, indicating the energy needed to drive the membrane for a single cycle, which is a lot higher compared to the case where the bioreactor can exchange air with the outside world (see Fig. 3.2).
Another system property is the pressure drop in the plastic air tubes. It is approximated as 4 kPa when the bioreactor operates cardiac cycles with high flows, see also Appendix C.

4.2 Aortic pressure control

The first bellows is position controlled on the cardiac cycle setpoint with a stroke of $40\ mL$, using a PI-controller and an ILC that works on the delayed setpoint $\tilde{r}_1$, as described in Chapter 3 (see Fig. 4.4a). The input u_2 controls a valve opening (5/3-way function), see section 2.2.1. A voltage $u_2 > 5V$ opens the compressed air supply port, while a voltage $u_2 < 5V$ connects the vacuum air supply port. For this first experiment, the equilibrium voltage is fed into the actuator of bellows 2, i.e. $u_2 = 5V$. In this way, the second bellows is not actuated, and 'dances' along with the movement of the first bellows, see Fig. 4.4b. The negative of setpoint $\tilde{r}_1$ is also displayed in this figure, to show how the bellows moves in anti-phase with the first bellows. The response of P_{ao} due to the movement of bellows 1 ranges from -2 to $19\ kPa$, see Fig. 4.4c.

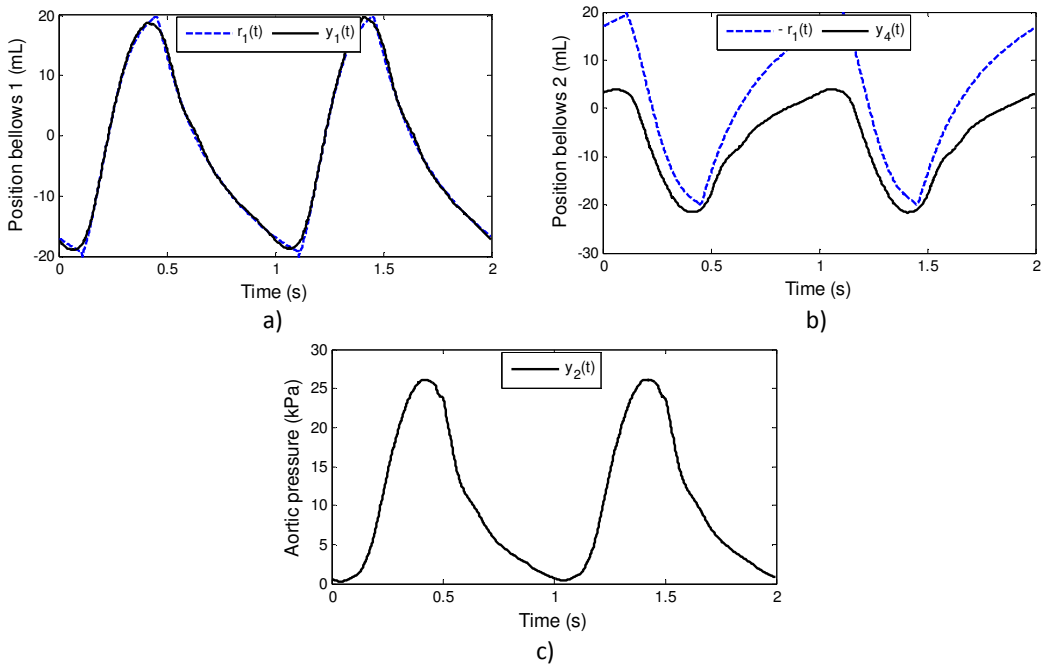

Fig. 4.4: Position control on bellows 1 (a), the response of the uncontrolled bellows 2 (b), and the response in the aortic pressure (c)

4.2.1 Constant pressure setpoint

In this section control strategies for bellows 2 to control the pressure P_{ao} are introduced and evaluated using an experiment. The goal is to control the pressure as shown in Fig. 4.4c to follow a constant setpoint of $\tilde{r}_2(t) = 12\ kPa$. Because the movement of the first bellows has a large influence on this pressure, it has to be taken into account to construct u_2. The system is too slow to be able to control P_{ao} merely by control on the pressure error $\tilde{e}_{22} = \tilde{r}_2 - y_2$. (The setpoint $\tilde{r}_2 = r_2\big(t - \tau_1(t)\big)$ results from delaying the original setpoint as described in section 0.) Therefore some other control approaches that use the movement of bellows 1 are introduced:

1. For the first approach, bellows 2 is position controlled to follow setpoint $\tilde{r}_4 = -\tilde{r}_1 + I_p \int \tilde{e}_{22}\, dt$. This setpoint is based on the negative of $\tilde{r}_1$, so that both bellows make the exact same movement, only in opposite direction. Furthermore, the setpoint is shifted using an weak integral action I_p, to obtain a correct pressure average. An ILC and PI-controller minimize the error $\tilde{e}_{44} = \tilde{r}_4 - y_4$. The resulting pressure response is not constant, and has pressure errors $|\tilde{e}_{22}| > 8\ kPa$, see Fig. 4.5a.
2. The non-equilibrium voltage of input u_1 is used to construct input u_2. In this way, actuator 1 behaves as master, while its behavior is copied to actuator 2 in order to obtain a constant pressure. To achieve the correct pressure level, an integral action I_p is used. Together this results in $u_2 = -K_{u_1}(u_1 - 5) + I_p \int \tilde{e}_{22}\, dt$, where $5V$ is the equilibrium voltage and the gain $K_{u_1} = 1$ to exactly copy the control signal. A better performance is obtained, with errors $|\tilde{e}_{22}| < 3\ kPa$, see Fig. 4.5b.
3. Proportional feedback on the pressure is added to the previous approach. The system is too slow to successfully suppress the pressure errors, see Fig. 4.5c.
4. Starting with approach 2, and ILC controller is implemented to work on error $\tilde{e}_{22}$. This controller is able to reduce pressure errors $|\tilde{e}_{22}| < 1.1\ kPa$, see Fig. 4.5d.

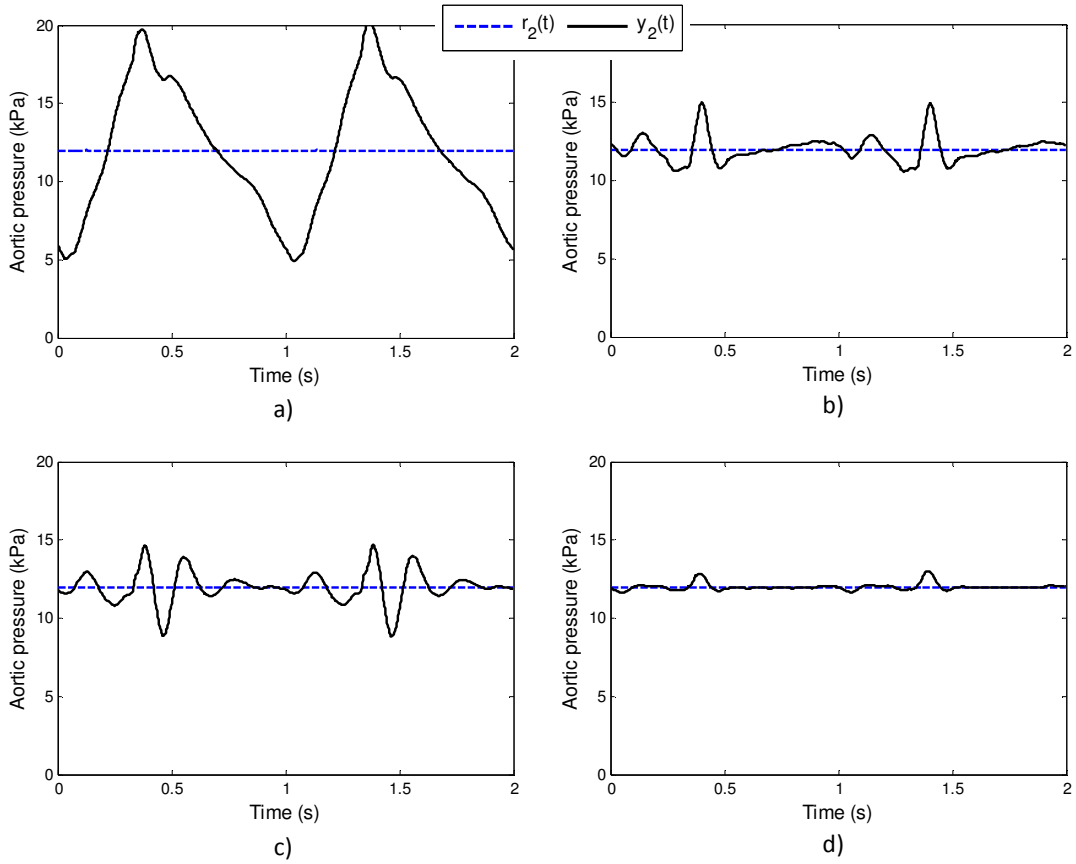

Fig. 4.5: Bellows 2 is dedicated to aortic pressure control, by minimizing $\tilde{e}_{44}$ (a), using input u_1 (b), using u_1 and a proportional action on $\tilde{e}_{22}$ (c) and using u_1 and an ILC on $\tilde{e}_{22}$ (d)

4.2.2 Cardiac cycle pressure setpoint

The next step is to replace the constant pressure setpoint with the setpoint for culturing heart valves (Fig. 1.2). The dashed line in Fig. 4.6 shows two cycles of this cardiac setpoint, that ranges between 10 and 16 kPa. We start with the second approach from the previous section, and obtain the results visualized in Fig. 4.6a. Reducing gain K_{u_1} results in the second bellows moving along with the first, but with a smaller amplitude. A profile in the aortic pressure arises naturally, with a shape resembling the cardiac cycle. Adjusting gain $K_{u_1}(= 0.68)$ results in the desired amplitude, see Fig. 4.6b. Next, an ILC algorithm on the pressure error $\tilde{e}_{22}$ is enabled, see Fig. 4.6c. Due to the difference in magnitude of compressed air supply P_c and vacuum air supply P_v (in general $|P_c/P_v| > 1$), the voltage u_1 above and below the equilibrium is corrected with scaling factor $|P_c/P_v|$. Finally, the control law

$$\begin{aligned} u_1 &= P\tilde{e}_{11} + I_p \int \tilde{e}_{11}\, dt + ILC(\tilde{e}_{11}) \ , \\ u_2 &= -K_{u_1}\left\{\max(u_1 - 5\ , 0)\left|\frac{P_c}{P_v}\right| + min(u_1 - 5\ , 0)\left|\frac{P_v}{P_c}\right|\right\} + I_p \int \tilde{e}_{22}\, dt + ILC(\tilde{e}_{22})\ , \end{aligned} \tag{4.1}$$

prescribes two inputs (see Fig. 4.6d), to control the two outputs, resulting in a fairly good performance. The position error of the driving bellows $|\tilde{e}_{11}| < 1.6\ mL$ and the pressure error $|\tilde{e}_{22}| < 1.1\ kPa$.

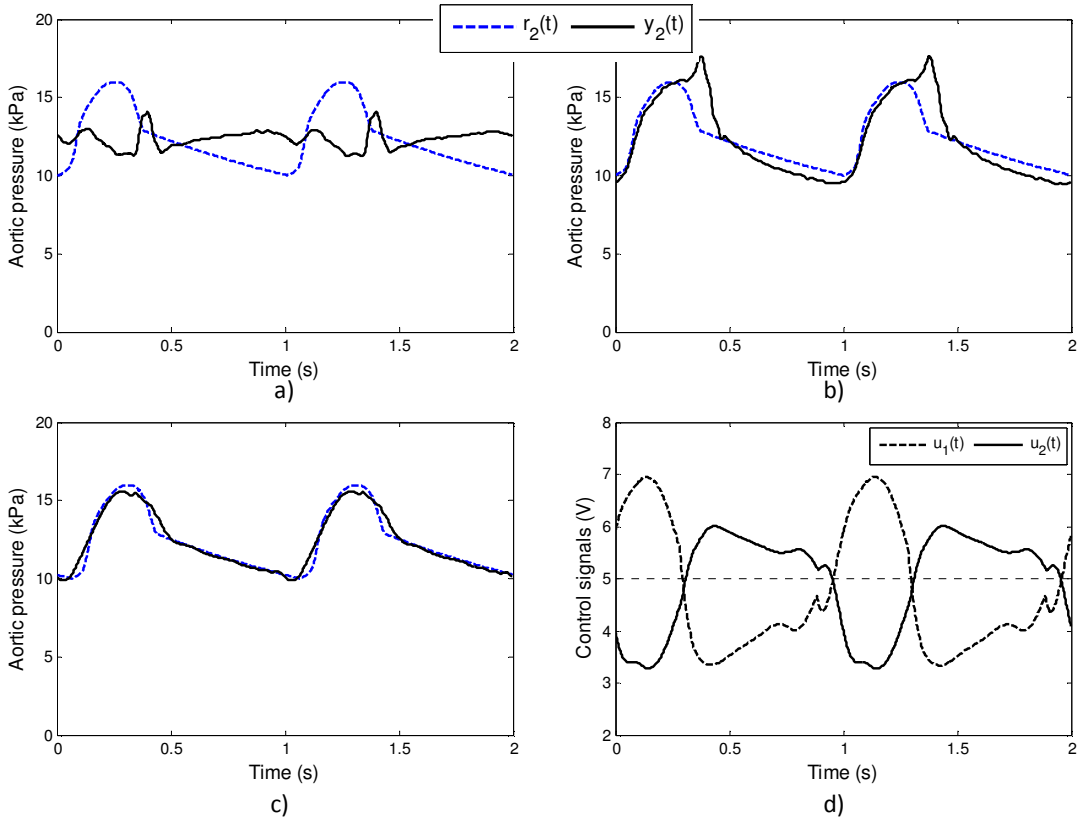

Fig. 4.6: Control of P_{ao} by using input u_1 (a), reducing the gain K_{u_1} (b), and enabling the ILC algorithm (c). The accompanying control signals (d)

4.3 Control of bypass valve

So far two inputs have been considered. In this section, the control voltage u_3 for the bypass steering valve (Fig. 2.3) actuator is addressed. The output pressure of this actuator is proportional to the voltage u_3. When this output pressure is approximately $18\ kPa$ higher than the internal bioreactor pressure (P_{ao}), the stiffness of the steering valve is overcome, and the valve is pushed down on its opposite tube connection. Increasing the actuating pressure results in a closing pressure that imposes a resistance in the flow through that tube connection (see also section 2.3). During systole, the bypass valve is entirely closed and no flow is possible through the bypass. In the diastolic phase the bypass valve is slightly opened, and the resistance on the back flow introduces a pressure difference $dP = P_{ao} - P_{lv}$. The magnitude of this valve closing pressure is an important control objective since this is the force imposed on the tissue. It is also the most difficult control objective for it is highly dependent on the properties of the culturing tissue heart valve, which change during the culturing process. Also, actuating the bypass changes the entire system dynamics, which makes it more difficult to correctly control P_{ao}. By increasing the actuation pressure on the bypass, while controlling P_{ao} as described in the previous section, dP during diastole is increased and thus P_{lv} is decreased. The controller for the bypass actuator therefore uses a weak integral action I_b to bring the minimum of P_{lv} during the diastolic phase ($\widetilde{P_{lv}}$) approximately to $0\ kPa$, i.e. $u_3 = I_b \int 0 - \widetilde{P_{lv}}\, dt$. This controller, together with inputs (4.1) but without the ILC for P_{ao} is used in an experiment that results in the cardiac pressures displayed in Fig. 4.7.

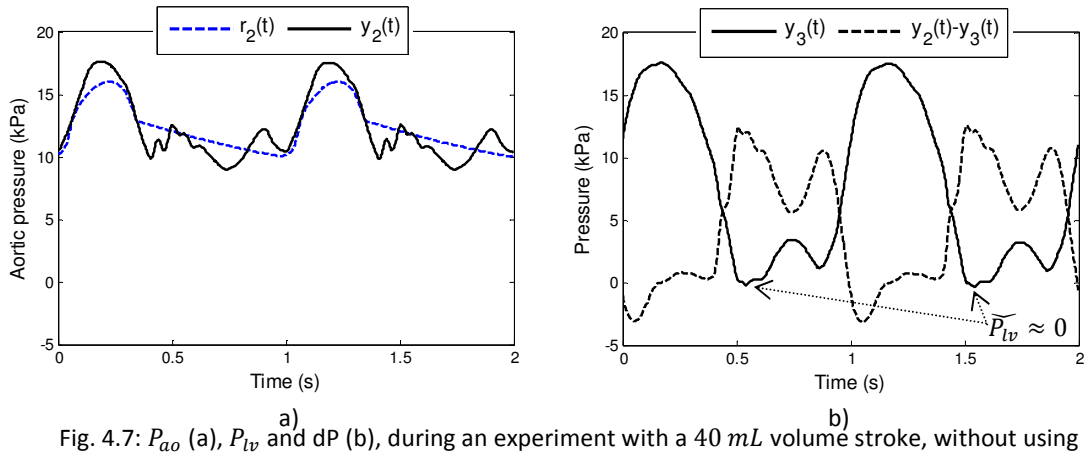

Fig. 4.7: P_{ao} (a), P_{lv} and dP (b), during an experiment with a $40\ mL$ volume stroke, without using ILC on the pressure error.

Without actuating the bypass, $P_{lv} \approx P_{ao}$. Fig. 4.7 shows a pressure difference arising successfully because actuating the bypass results in $\widetilde{P_{lv}} \approx 0$. To improve tracking performance of P_{ao}, the pressure ILC is enabled. Care has to be taken, because the system can become unstable. The pressure oscillation at the end of the systolic phase is a natural reaction due to the closing of the heart valve and therefore not necessary to suppress. Therefore, the ILC algorithm is enabled, but only at the remaining part of the signal, denoted by the shading in Fig. 4.8a. The learning rate is higher in the systolic phase than in the diastolic phase, because the resistance of the bypass on the flow during diastole causes pressure oscillations that are hard to suppress. A large learning rate could make the system unstable, when the ILC is not exactly synchronized; the timing of the ILC signal playback is important to be exactly synchronized with system delays. Together with the phase delay of the lowpass filters, the pneumatics and electronics contribute to this total system delay.

The negative peak (approximately $-3\ kPa$) in the pressure difference is needed to unfold and open the test valve from its firmly closed position. This is typical for the TPU test valve used.

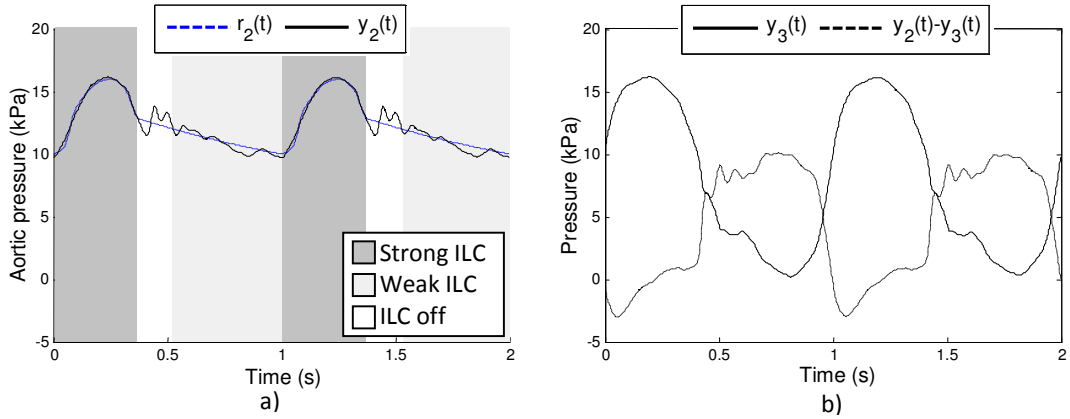

Fig. 4.8: P_{ao} (a), P_{lv} and dP (b), during an experiment with a $40\ mL$ volume stroke, using an ILC controller whose learning rate changes depending on the cardiac phase.

Similar experiments are performed with stroke volumes of 20 and $60\ mL$, see appendix D. A summary of the maximum errors is provided in Table 4.2. For the pressure error a distinction is made where the ILC is on or off.

Table 4.2: Maximum errors of the MIMO experiments

Stroke (mL)	$max\|\tilde{e}_{11}\|\ (mL)$	$max\|\tilde{e}_{22}\|\ (kPa)$ ILC on	ILC off
20	1.3	0.6	1.1
40	1.6	0.8	1.4
60	2.1	1.1	2.2

4.4 Protocol functionality

The Simulink model contains an interface that allows adjustment of the volume setpoint (both stroke and profile) and pressure setpoints (amplitude, bias and profile). Also the cycle frequency and the desired pressure difference can be changed, or preprogrammed to change gradually in time by setting timeline markers. At different combinations of setpoint parameters, a set of controller gains is tuned for optimal performance and stored in the Simulink model. When the user changes the setpoint, the set of gains is obtained by interpolating between these preprogrammed sets. Different operating modes are programmed in protocols. For instance, the user can choose the protocol where only the bellows position is controlled, or the protocol where both position and pressure are controlled, but without imposing a pressure drop on the heart valve using the bypass. The default protocol is the '*automatic protocol control*', where the system switches between the '*startup*' protocol and the '*normal run*' protocol. In the *startup* protocol, the position of the bellows is slowly controlled to go to a predefined position. The ventilation valve is open, in order to allow fluid exchange from the nutrient fluid supply chamber (Fig. 2.9). When the bellows arrive at the correct position and both the pressures P_{ao} and P_{lv}

are close to zero (defined as atmospheric pressure), the system switches to the *normal run* protocol. The ventilation steering valve closes, and gradually the amplitude in the position setpoint of bellows 1 is increased (similar to Fig. 4.3). When the position ILC converges and the controller achieves a steady state, the P_{ao} setpoint bias is gradually brought from $0\ kPa$ to the value set by the user and the pressure ILC starts its updating procedure. Finally, the bypass actuation pressure is slowly increased until the desired pressure drop over the heart valve is obtained. The first two controllers automatically readjust to the severely changed system dynamics due to the bypass. After a few minutes the system reaches a steady operating cycle. The *automatic protocol control* sometimes resets the system using the *startup* protocol, and goes back to *normal run* again. The following events can trigger the system to restart:

- A safety system monitors the maximum internal pressures and the position of the bellows. If a certain threshold is crossed, the system restarts. If for some reason this restart does not help immediately and even higher thresholds are crossed, the entire simulation stops. Simulation stop causes the pump to shut down immediately, using a solid state relay. This relay also opens two pressure valves that release the remaining pressure inside the tubes. These valves are installed to ensure total protection of the bioreactor.
- The system detects leakage (analogue to 'Haemorrhage') by monitoring the bias of the bellows 2 movement. When the system leaks, this bellows moves inwards to maintain internal pressure. When it moves too far inwards, the system restarts and subtracts nutrient fluid from the supply chamber to compensate for the leakage.
- Switching back to the startup protocol also allows for refreshment of nutrient fluid, by fluid exchange with the supply chamber. Fluid exchange can be requested manually, or programmed to occur on predefined intervals.
- When setpoint changes are made by the user, the system resets and gradually restarts.

CHAPTER FIVE

Conclusions and future work

5.1 Conclusions

Using the knowledge obtained from the prototype feedback system, a bioreactor setup was established that is both accurate and reliable. It uses ultrasonic sensors, pressure sensors and a pneumatic actuation system consisting of pressure regulators and control valves.

Experiments were performed where a single bellows was controlled on its position, with the bioreactor opened to the outside world. They provided a basis to test different control strategies, and an intuitive understanding of the system properties was obtained. From a control point of view, the bellows is the most important component of the bioreactor. Due to the improved bellows design, the ultrasonic sensor is able to follow the bellows position at all time. A proportional-integral (PI) controller combined with an iterative learning controller (ILC) reduced tracking errors for a $20\ mL$, $40\ mL$ and $60\ mL$ volume stroke to $1\ mL$, $1.6\ mL$ and $1.9\ mL$ respectively. The ILC approach was effective because of the repetitive character of the cardiac cycle. Due to changing system dynamics, the ILC signal has to be reestablished frequently, and restarting the system is not an option while culturing heart valves. A lowpass filter for the ILC signal provides enough robustness to allow the ILC signal to be updated online. The system contains considerable delays due to phase delay, the dynamics of the sensors, actuator, electronics, and the pneumatic system. This delay is allowed, as long as the cardiac conditions are resembled. Therefore the PI-controller acts on the error based on the original setpoint, while the ILC acts on the error based on a delayed setpoint. This variable delay is estimated online, aimed at optimally fitting the delayed reference on the measurements.

For the pressure control experiments, the bioreactor was closed to the outside world. Bellows 1 was controlled on its position, while bellows 2 was used to control the aortic pressure, by copying the behavior of the actuator for bellows 1 to the actuator for bellows 2. An integral action was used to achieve the correct pressure level and a pressure ILC controller was implemented to reduce the repetitive part of the error, resulting in a maximum pressure error of $1.1\ kPa$, while using a volume stroke of $40\ mL$.

To test full operating mode, a TPU test heart valve was installed to resemble a tissue heart valve. The bypass steering valve was used to achieve a closing pressure on this tissue valve, by imposing a resistance on the flow back to the first membrane. This severely changes system dynamics, and the first two control inputs have to readjust to this change. All three controllers have a large influence on one another. Therefore a clear distinction is made in the strength of the three controllers. The first actuator is most dominant, and controls the first ('driving') membrane strongly on its position. The second actuator follows part of the first actuator's motion, assisted by a slow pressure ILC controller. The learning rate of this ILC changes depending on the phase of the cardiac cycle, because for instance the pressure oscillation due to the closing heart valve does not have to be suppressed. The bypass controller only uses a low integral action giving the first two controllers time to readjust to the changing system dynamics. A fourth actuator is merely responsible for opening and closing the nutrient fluid supply chamber.

The focus of the control system is not to achieve high performance very fast, but the priority is preventing large pressure oscillations and aggressive flows that could damage the tissue heart valve.

The designed control system enables the disposable bioreactor to achieve all necessary functionality for cultivating heart valves during the growing, conditioning and testing phase.

5.2 Future work

Four fully mobile stand-alone bioreactor setups where build. One of them is presently being used in 'cellab' [4], for the group *soft tissue Biomechanics & Tissue Engineering*, department of Biomedical Engineering, Eindhoven University of Technology. The disposable parts have past toxicity and sterilization tests. A new chapter starts for the bioreactor project, which brings about some new issues and points of interest:

- Because the bioreactor will be placed inside an incubator, it is subject to higher temperatures and system dynamics will change. Most likely this has a positive effect on controllability because the membranes become more flexible. Nonetheless the sets of gains for different operating modes have to be adjusted.
- To improve performance the possibilities of gain scheduling should be investigated.
- Work has to be done to further improve the usability of the user interface, with an accompanying user manual. A visual tool for long term setpoint planning and nutrient fluid exchange planning is among these improvements.
- Automatic image analysis in the loop, using the high speed camera, can provide estimates of the heart valve deformation and other mechanical properties. These properties should be used to adjust the system operation.

Appendix A Bioreactor set-up

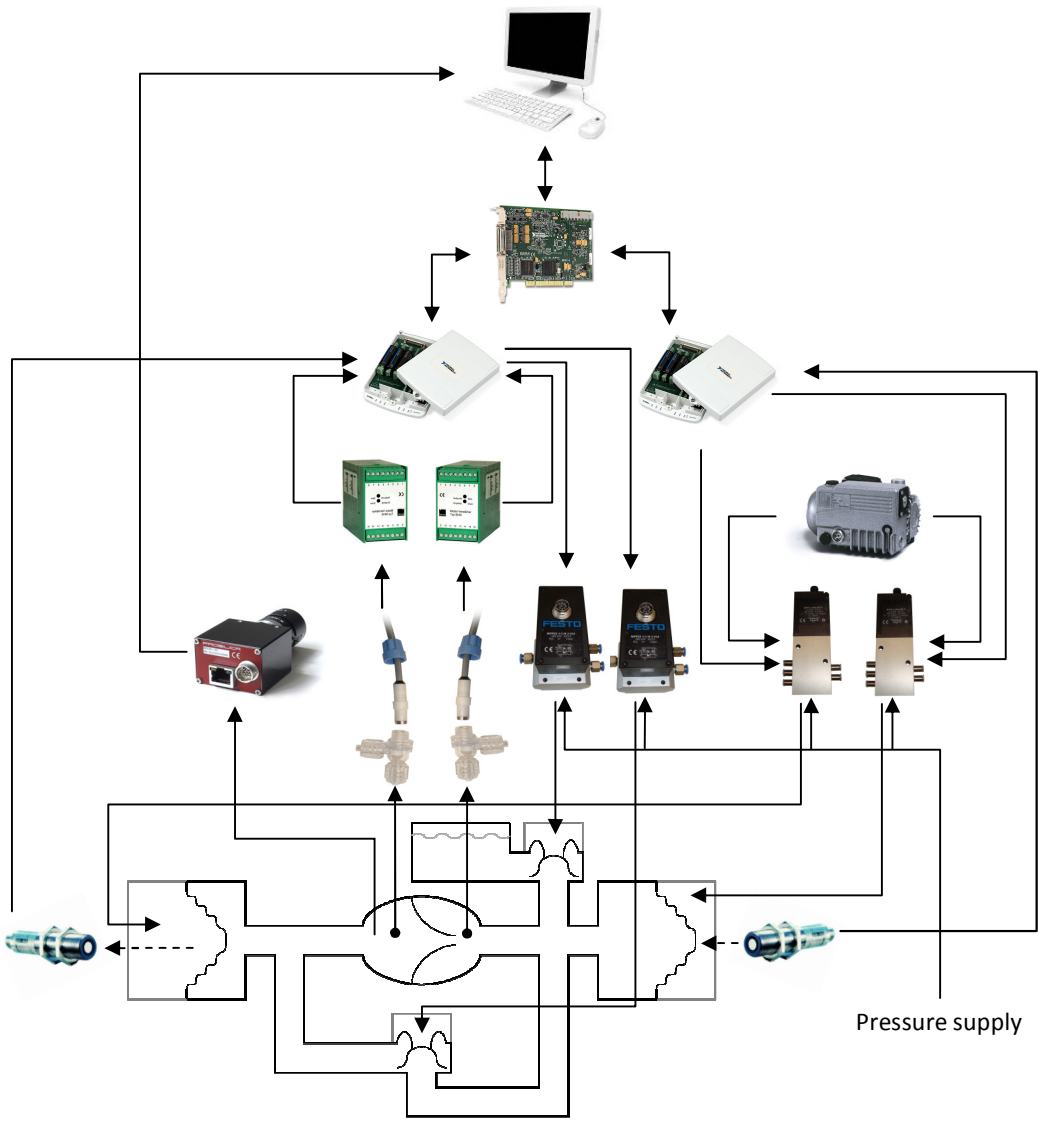

Fig A.1: Schematic representation of all system components

Fig A.2: The entire bioreactor set-up was reproduced four times. Every setup is build inside a mobile PC-working station

Fig A.3: The electronic and pneumatic components are mounted on a plate attached to a sliding drawer

Fig A.4: Impression of the reproduction stage

Appendix B Position control experiments

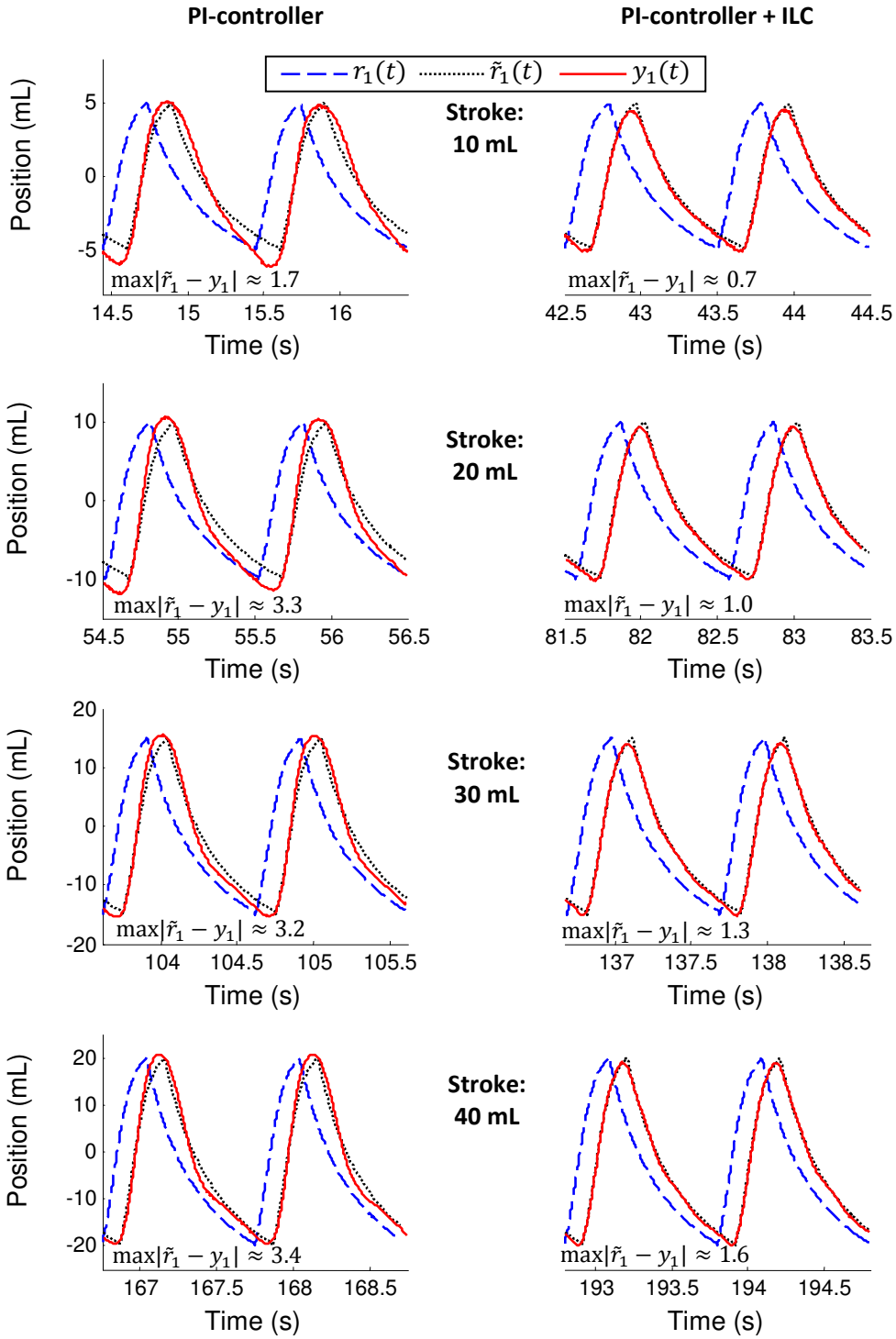

Fig B.1a: Position control experiments on bellows 1.
The left figures, where only a PI-controller is used, show repetitive errors. In the right figures where the ILC algorithm is enabled, these errors are suppressed.

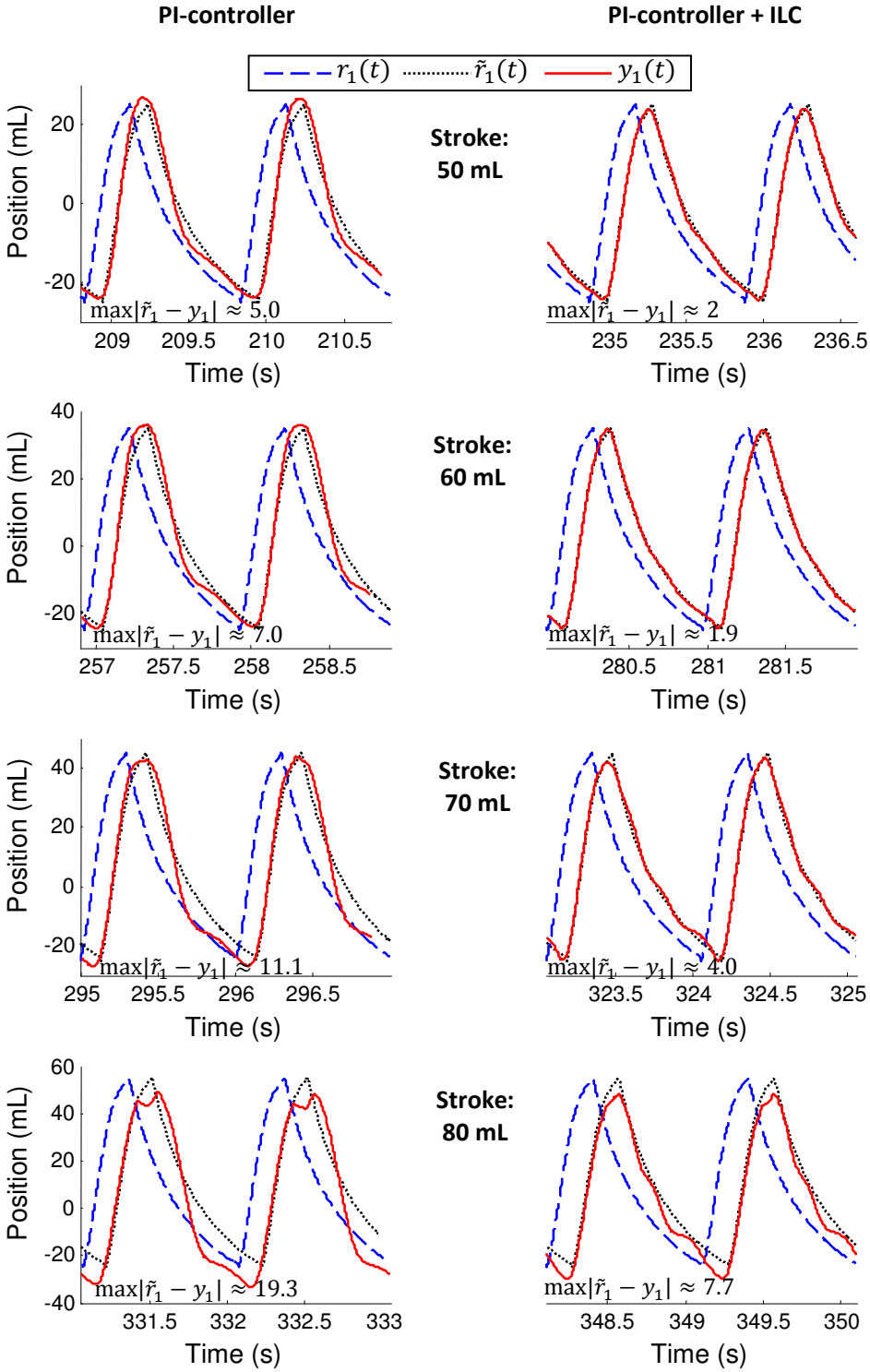

Fig B.1b: Position control experiments on bellows 1
For high stroke volumes

Appendix C Pressure drop through plastic tube

The bioreactor is actuated using pressure control valves that are connected with long plastic tubes, that have an inner diameter of $d = 4mm$. The magnitude of the pressure drop of the air flow through such a tube is estimated analytically and using two experiments.

Analytic approximation

In order to calculate the pressure drop, the Reynolds number is calculated for different flow rates. The Moody diagram is used to approximate the accompanying friction factor f. The pressure drop per meter tube is than calculated using $\frac{\Delta p}{l} = \frac{1}{2}\rho v^2 \frac{f}{d}$, where ρ is the density of air. The speed of the air v is related to the flow rate and the cross-sectional area of the tube. The relation between the pressure drop per meter and the flow rates is displayed in Fig. C.1. The part corresponding to the transition region between laminar and turbulent flow is omitted.

Experiments

To measure the pressure drop in the tube, for different air flow rates, the bioreactor itself is used as a flow meter. The bellows is position controlled to follow a few cycles of a certain setpoint. A plastic tube of exactly 2 meter is placed between the actuator and the bioreactor. The pressure just before and just after this tube is measured. The pressure difference is related to the air flow inside the tube, which is obtained by taking the derivative of the displacement of the bellows, measured using the ultrasonic sensor. The 2 meter tube is replaced by a 4 meter tube, and the experiment is repeated. The pressure drop measurements per meter tube are calculated and compared in Fig. C.1.

The experimental values are slightly higher than expected compared to the analytic approach. The experimental accuracy is questionable. Also the pipe roughness may be higher than assumed in the analytical approximation. As a conclusion, the pressure drop is approximated as 4 kPa when the bioreactor operates cardiac cycles with high flows.

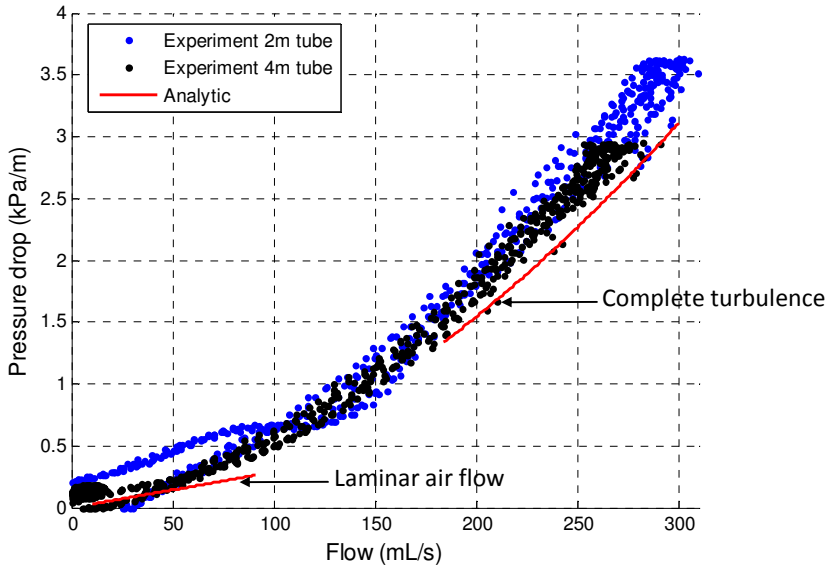

Fig C.1: Pressure drop of air flow per meter plastic tube

Appendix D Final results

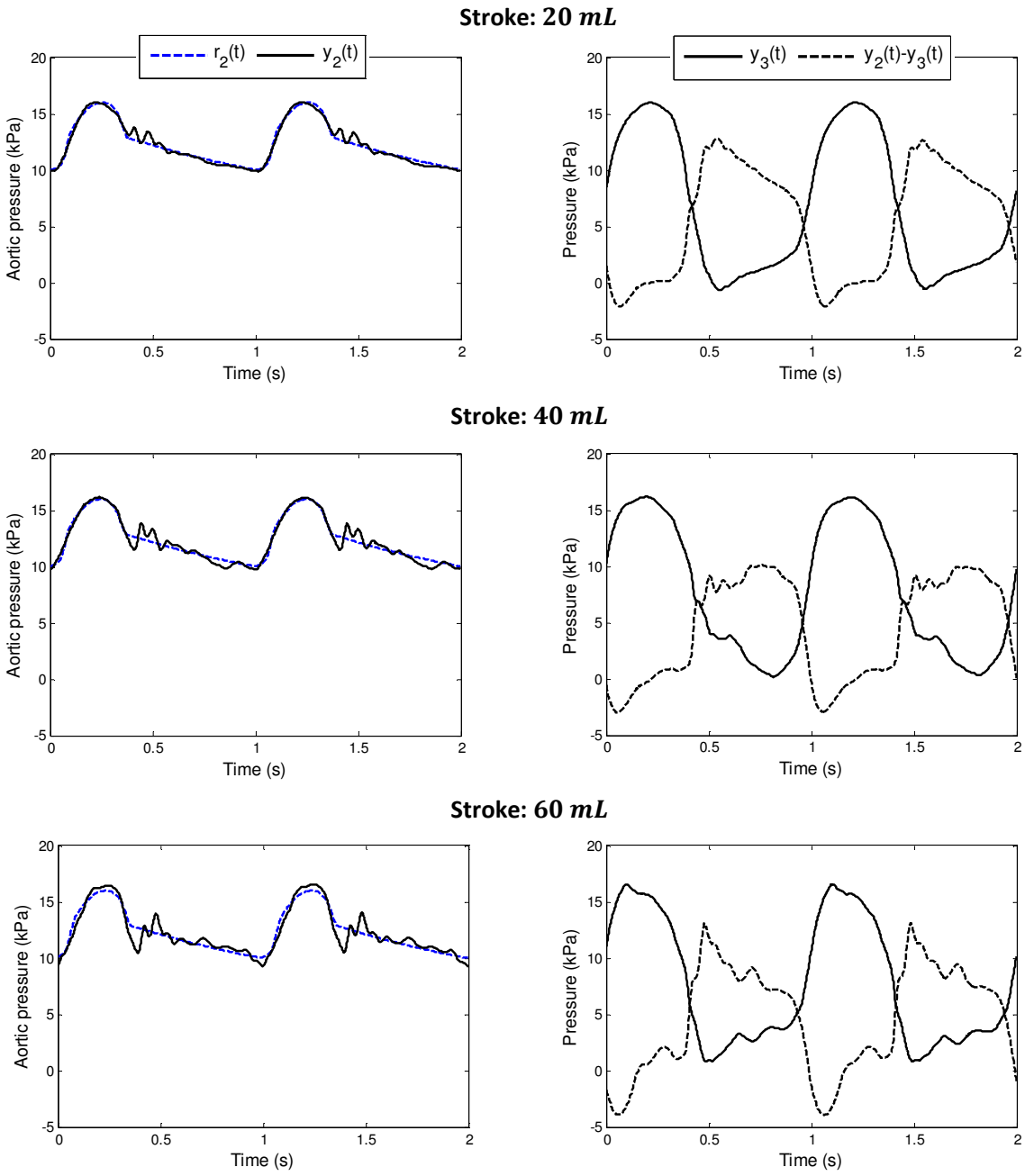

Fig D.1: The final results with volume strokes 20, 40 and 60 mL, the position is controlled as described in chapter 3, the pressures as described in chapter 4. The figures only visualize the measured pressures; the performance in position of bellows 1 is comparable to the figures of appendix B.

Appendix E Simulink model and Graphical User Interface

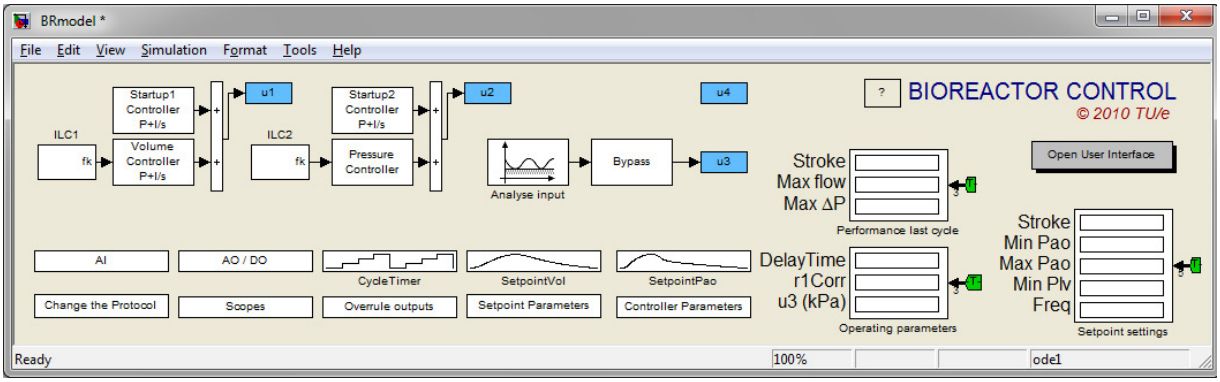

Fig E.1: The main screen of the Simulink model

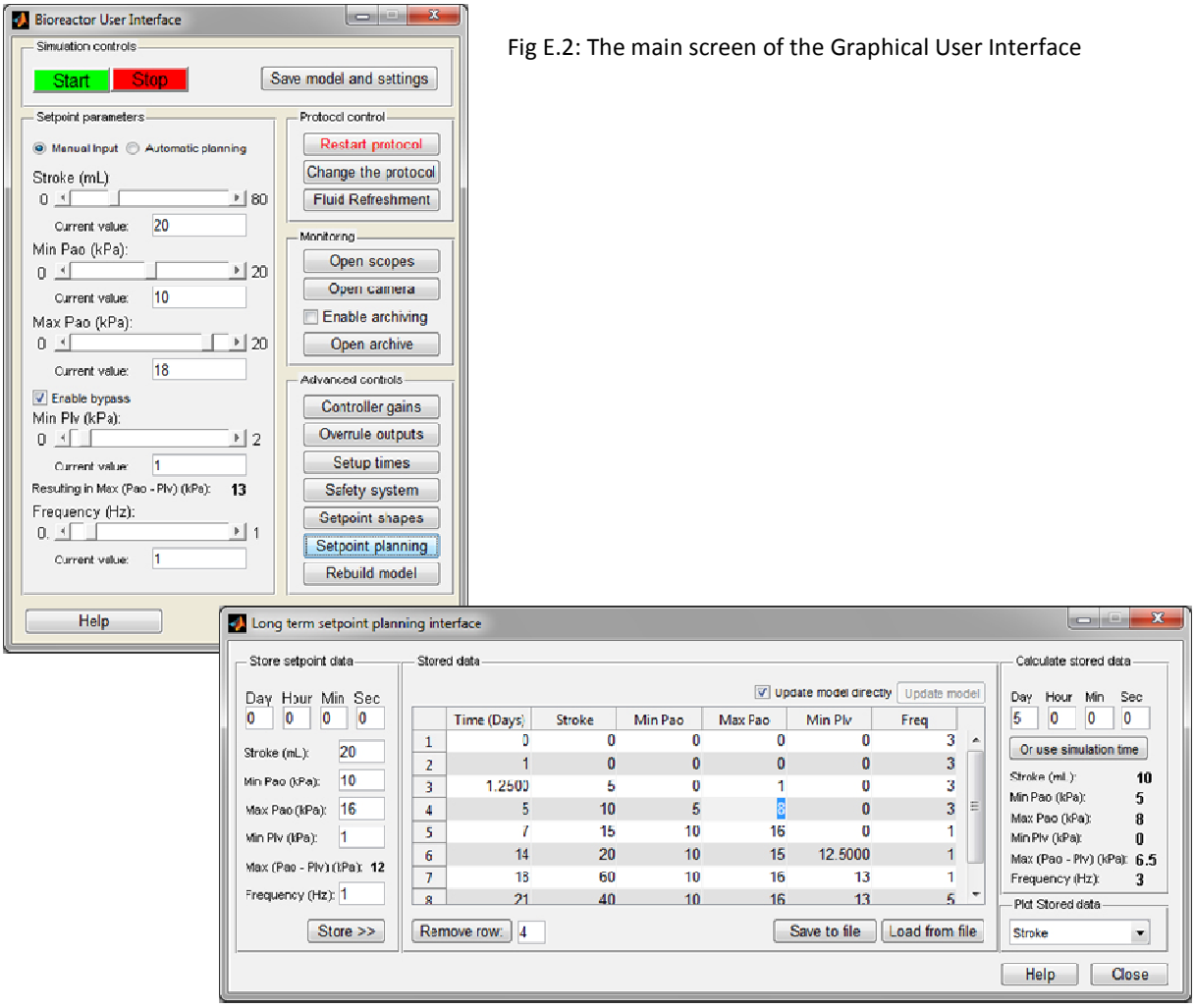

Fig E.2: The main screen of the Graphical User Interface

Fig E.3: The Graphical User Interface for long term setpoint planning

Bibliography

[1] Baaijens, F. P. T., Bouten, C. V. C., Mol, A., Rutten, M. C. M., Hoerstrup, S. P., European and U.S. Patent 0 145 920 A1 (2008)

[2] Banerjee, A. G., et al., "Incorporating Manufacturability Considerations during Design of Injection Molded Multi-material Objects", Res. Eng. Des., 17, 207–231 (2007), DOI:10.1007/s00163-007-0027-9

[3] Becton Dickinson, "Miniature Pressure Transducer, model P10EZ", www.bd.com (2010)

[4] Biomechanics and Tissue Engineering , www.mate.tue.nl/mate/research/index.php/2 (2010)

[5] Biomedical Brochure, Tissue Engineered Heart Valve, www.tue.nl (2007)

[6] Burster, "Amplifier Module, model 9243", www.burster.com (2010)

[7] Driessen Mol, A., et al., "Tissue Engineering of Semi-lunar Heartvalves, Current Status and Future Developments", Journal of Heart Valve Desease, 13, 272–280 (2004)

[8] Driessen Mol A., et al., "Tissue Engineering of Human Heart Valve Leaflets: A Novel Bioreactor for a Strain-based Conditioning Approach", Annals of Biomed. Eng., 33, 1778–1788 (2005), DOI:10.1007/s10439-005-8025-4 PMid:16389526

[9] Dumont, K., et al., "Design of a New Pulsatile Bioreactor for Tissue Engineered Aortic Heart Valve Formation", Artificial Organs, 26(8), 703–733 (2002), DOI:10.1046/j.1525-1594.2002.06931_3.x PMid:12139499, Eindhoven University of Technology, Eindhoven, The Netherlands,

[10] Festo, "Electronic proportional air flow valves", www.festo.com (2010)

[11] Fujinon, "35 mm lens, model HF35HA-1B", www.fujinon.com (2010)

[12] HemoLab B.V., Three Leaflet TPU Heart Valve (2009)

[13] Hoerstrup, S. P., et al., "New Pulsative Bioreactor for in Vitro Formation of Tissue Engineered Heart Valves", Tissue Eng., 1(6), 75–79 (2000a), DOI:10.1089/107632700320919 PMid:10941203

[14] Hoerstrup, S. P., et al., "Functional Living Trileaflet Heart Valves Grown in Vitro", Circulation, 102(19), 44–49 (2000b)

[15] Horst-Witte, "Vacuum pump model 95969", www.horst-witte.de (2010)

[16] Human heart and aortic valve: www.myhealth.com, Healthwise

[17] Kok, T. "Control engineering of a disposable bioreactor", Master Thesis, DCT 2007.031, Eindhoven University of Technology, Eindhoven, The Netherlands (2007).

[18] Kortsmit, J., "Non-invasive Assessment of Leaflet Deformation and Mechanical Properties in Heart Valve Tissue Engineering", PhD Thesis, Eindhoven University of Technology, Eindhoven, The Netherlands (2009)

[19] MaTe, "Infrastructure." www.mate.tue.nl (2010)

[20] The MathWorks, "Real-Time Windows Target 3.5", www.mathworks.com

[21] Microsonic, "Ultrasonic Sensor model LPC 25", www.microsonic.de (2010)

[22] Mol, A., "Functional Tissue Engineering of Human Heart Valve Leaflets", PhDThesis, Eindhoven University of Technology, Eindhoven, The Netherlands (2005)

[23] National Instruments, "Multifunction Data Acquisition model PCI-6229", www.ni.com (2010)

[24] Neerincx, P.E., Meijer H.E.H., "Design, realization and optimization of a disposable bioreactor for growing, culturing and testing of tissue-engineered heart valves", International Polymer Processing, 25(2), 1-10, (2010)

[25] Norgren, “Electronic proportional air flow valves”, www.norgren.com (2010)
[26] Peterson, A., Landeen, L. K., Bennett, J., Gee, J., Chesla, S., Zeltinger, J., U. S. Patent 5 846 828 (1998)
[27] Peekel Instruments, “Picas Measuring Amplifier”, www.peekel.nl (2010)
[28] Prosilica, “High speed camera, model GC640C”, www.prosilica.com (2010)
[29] Qosina, “Disposable components”, www.qosina.com (2010)
[30] Rubbens, M. P., “Mechano-regulation of Collagen Architecture in Cardiovascular Tissue Engineering”, PhD Thesis, Eindhoven University of Technology, Eindhoven, The Netherlands (2009a)
[31] Rubbens, M. P., et al., “Intermittent Straining Accelerates the Development of Tissue Properties in Engineered Heart Valve Tissue.” Tissue Eng., 15(5), 999–1008 (2009b), DOI:10.1089/ten.tea.2007.0396 PMid:18795866
[32] Rutten, M. C. M., et al., “The Valve Exerciser: A Novel Bioreactor for Physiological Loading of Tissue-engineered Aortic Valves”, J. Biomech., 32, 1039–1049 (2005)
[33] Siglab, “Dynamical signal analysis system”, www.acoutronics.com (2010)
[34] Stanuszek, M., “FE Analysis of Large Deformations of Membranes with Wrinkling”, Finite Elem. Anal. Des., 39, 599–618 (2003), DOI:10.1016/S0168-874X(02)00130-0